8-22-2023 11:30 AM

Changes in peatland soil fauna biomass alter food web structure and function under warming and hydrological changes

Trevor L. Pettit, *Western University*

Supervisor: Lindo, Z., *The University of Western Ontario*

A thesis submitted in partial fulfillment of the requirements for the Master of Science degree in Biology

Abstract

Short-term climate perturbations affect both predator and prey species that comprise soil communities, and alter carbon flux. I used a mesocosm experiment to model the effects of experimentally-imposed temperature and moisture conditions that simulate potential future conditions during climate perturbations, on peatland soil food web flux and soil carbon sequestration after three-weeks of experimentally imposed conditions, and then again after an additional three-week recovery under control conditions. I compared system resistance and resilience, and modelled carbon (C) and nitrogen (N) fluxes throughout the mesocosm experiment. There was a lack of resistance of the soil food web to perturbation shown by changes in total faunal abundance under imposed soil moisture treatments. System resistance and resilience are important concepts to understand as climate change threatens C storage in boreal peatlands, a globally significant C store.

Keywords

carbon flux, nitrogen mineralization, soil biodiversity, boreal peatlands, energetic food web models, hydrological changes, warming

Summary for Lay Audience

Carbon (C) makes up the substrate, habitat, and diet of soil-dwelling organisms. Therefore, soil food web C storage is defined by the total amount of C consumed by soil fauna less the total C released to the atmosphere by the respiration of soil fauna. Short-term changes in temperature and soil moisture affect the storage of C in soils. Boreal peatlands are a wetlands ecosystem found across Canada that play an especially important role in global C storage. The goal of my thesis was to determine the effects of potential future temperature and soil moisture conditions on the total number of soil fauna, the total amount of C consumed by soil fauna, and the total C released to the atmosphere by the respiration of soil fauna before the simulated short-term event, immediately following the event, and then following a subsequent recovery period under control conditions in peat-soils collected from White River, Ontario. Overall, the total number of soil fauna tended to decrease following the simulated event, and this was driven by imposed soil moisture treatments. The total number of fauna did not increase following the recovery period, and this was most noticeable in the number of fungal-feeding soil fauna. System resistance and resilience are important concepts to understand as climate change threatens C storage in boreal peatlands, a globally significant C store.

Co-Authorship Statement

In the following thesis, the soil fauna abundance, biomass, and food web modelling following three-week perturbation (i.e., T_1 data) was published in a Special Issue on soil food web (Pettit et al. 2023):

> Pettit, T., Faulkner, K.J., Buchkowski, R.W., Kamath, D., and Lindo, Z. (2023) Changes in peatland soil fauna biomass alter food web structure and function under warming and hydrological changes. European Journal of Soil Biology 117: 103509. https://doi.org/10.1016/j.ejsobi.2023.103509

TP, KJF and ZL conceived the experiment; TP and KJF performed the field sampling and experiment; TP identified and enumerated the mesofauna samples; DK enumerated the microfauna subsamples; TP generated the biomass data, and performed the food web analysis; RWB wrote the code for the food web model; TP wrote the draft of the manuscript with input from ZL; all authors contributed to the final version of the article.

Acknowledgments

I thank Dr. Zoë Lindo for the support and help through both my undergraduate and graduate research projects. Thank you for always keeping me on track over our many weekly one-on-ones, both virtually and otherwise. Also, thanks to Dr. Brian Branfireun for allowing me to use the facilities in his lab for my research and guidance in the field.

I also thank my advisors, Dr. Keith Hobson and Dr. Yolanda Morbey. Your feedback and flexibility are greatly appreciated! I especially thank Dr. Morbey for advising both my undergraduate and graduate research projects.

Thanks to all my Lindo Lab mates past and present for the tremendous help and numerous teardowns. I especially thank Dr. Katy Faulkner for help from the start through the end of the project and for always being available for questions. I also give special thanks to Dr. Rob Buchkowski for years' worth of help troubleshooting and for helping me develop my interest in modelling.

Finally, I thank my family and Sydney for their constant support.

Table of Contents

List of Figures

List of Appendices

Chapter 1

1 Introduction

1.1 Carbon Cycling in the Soil Food Web

Nearly 80% of all carbon (C) stored in terrestrial ecosystems (2500 GT of C) is found in soils (Batjes, 1996). Net primary production derived from aboveground photosynthesis drives the input of fixed C into soil systems as detritus (i.e., dead organic matter) which serves as the basal energy source for soil food webs (de Vries and Caruso, 2016). Carbon is then transferred from one trophic level (or trophic group) to another via consumption during trophic interactions in an overall process that contributes to decomposition of detritus. At the same time, C transformations occur belowground as C is stored as living biomass, recycled to the detritus pool through feces and other consumptive waste, and as natural (non-consumptive) death of soil organisms. Carbon is lost from soils as carbon dioxide (CO_2) as a function of metabolic respiration by members of the soil food web (Moore and de Ruiter, 2012). Thus, the fate of soil C is a function of detrital inputs, the soil food web, and related heterotrophic respiration outputs (Figure 1.1).

The soil food web consists of several trophic levels and many taxonomic groups. The primary consumers (decomposers) of detritus are the microbial groups (fungi, bacteria, protists) that use C and other nutrients from detritus as well as root exudates to maintain biomass and metabolic function. Feeding on the microbes (secondary consumers/decomposers) are a wide variety of taxa that include microfauna (e.g., nematodes) and mesofauna (e.g., mites and collembola), while predators of the system are mainly other nematode and mite groups. Carbon is the main energetic currency for heterotrophic organisms, alongside nutrients (e.g., nitrogen (N)), that is transferred among members of the soil food web. However, the process of trophic transfer especially of C is inefficient (Hunt et al., 1989), as C is lost from the food web due to metabolic and other biological processes. Specifically, consumed C (and other nutrients) must first be assimilated (digested) so that energy is available for cellular processes including general metabolic maintenance as well as growth and reproduction. Assimilation efficiency (E_a) differs greatly among soil organisms (e.g., collembola E_a = 50% vs. nematode-feeding mites E_a = 90% (Moore and de Ruiter, 2012)), with unassimilated food released as waste products that return to the

detrital source pool. Assimilated C is then allocated to metabolic function or production (i.e., growth and reproduction). Following the Metabolic Theory of Ecology, metabolic functions for soil organisms are largely controlled by temperature (Brown et al., 2004), and C is lost as a by-product of metabolism as CO_2 via heterotrophic respiration. Production efficiency (E_p), which then defines the C allocated to growth and reproduction with metabolic waste released as respired CO_2, is a function of metabolic activity and also varies across different soil organisms (e.g., fungi E_p = 30% vs. protists E_p = 40% (Moore and de Ruiter, 2012)). Metabolism increases and thus production efficiency decreases with increasing temperature. Thus, changes in both the soil food web topology and metabolism (temperature) drive changes in soil C storage (Figure 1.1).

1.2 The Stability of Soil Food Webs

The stability of a system can be considered as two components (Allison and Martiny, 2008): resistance and resilience. Whether a system resists change under such a perturbation (resistance) and/or how fast a system recovers from a perturbation (resilience) when it does change are important parameters to understand how biodiversity may be altered under climate and other anthropogenic change. The extent to which a community biomass decreases immediately following a disturbance is indicative of the level of resistance (Hillebrand and Kunze, 2020); the faster recovery of community biomass following a disturbance is indicative of resilient communities (Griffiths and Philippot, 2013). The resistance of a community to a disturbance plays an important role in determining how long it will take a community to recover (Hillebrand and Kunze, 2020). The resistance and resilience of communities depends on several factors, including resource availability (Gessler et al., 2017), biodiversity (Isbell et al., 2015), and species traits (Gladstone-Gallagher et al. 2019). However, examples of stability, resistance and resilience are uncommon for whole soil food webs (but see de Vries et al., 2012).

There are several factors that suggest soil systems should show high levels of stability. First, soil food webs are complex systems characterized by many trophic groups (Digel et al., 2014) and high species richness within trophic groups (Verhoef and Brussaard, 1990). Soil food webs are also characterized by many complex interactions, including omnivory (Neutel et al., 2002), cannibalism (Moore and de Ruiter, 2012; Buchkowski et al., 2022), necrophagy (Luxton, 1972),

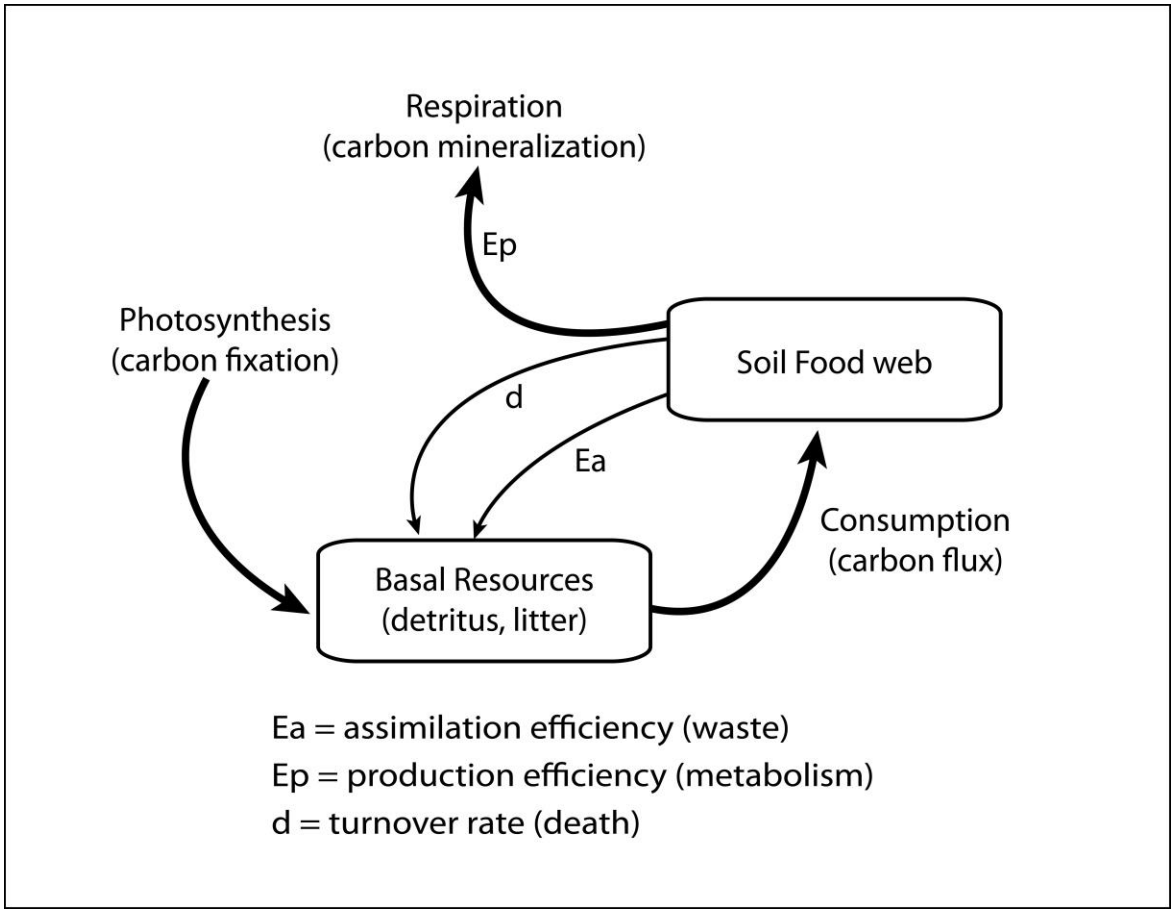

Figure 1.1 Conceptualized flow of carbon and nutrients through soil systems.

Carbon initially enters the soil system as detritus which is derived from aboveground photosynthesis and net primary productivity (I.e., carbon fixation). Detritus (dead organic inputs largely from aboveground sources) forms the basal resource for the soil food web. Detrital carbon and nutrients is transferred among members of the food web through consumption. Consumption drives fluxes of carbon within and between nodes in the soil food web. Carbon returns to the detrital pool through waste due to inefficient trophic assimilation (E_a) and through non-consumptive death (d) of soil organisms. Carbon is lost from the soil system through carbon mineralization, by which organic carbon is turned into inorganic (i.e., mineral) forms. In soils, carbon mineralization is largely heterotrophic respiration associated with metabolism of soil organisms (i.e., production efficiency, E_p). Soil carbon pools are both the detrital pool and the soil organisms themselves that comprise the soil food web.

and intraguild predation (Parimuchová et al., 2021). Complex interactions tend to be weaker than other consumer-resource interactions (i.e., direct predator – prey trophic transfer), which has been suggested to have greater stability than systems with fewer complex interactions (O'Gorman and Emmerson, 2009; LeCraw et al., 2014).

Soil food webs also tend to show a 'diamond' shaped trophic topology (McCann and Rooney, 2009) with two compartmentalized subwebs stemming from a basal resource and fed upon by a common top predator. This results in the soil food web having two discrete resource compartments or energy channels that form from lower-order consumers (bacteria or fungi) that tend to derive the bulk of their C from different aspects of the detrital pool (Rooney et al., 2006). These two energy channels support different microbial consumers, and the channels differ in production and turnover rate. The bacterial energy channel exhibits faster turnover than the fungal channel as indicated by greater production:biomass ratios in soil systems dominated by non-woody plants (Rooney et al., 2006) and when detrital inputs have low C:N ratios. The fungal energy has a slower turnover rate and is dominant when detrital inputs have high C:N ratios. Top arthropod predators such as predatory mites couple these distinct energy channels as their prey are consumers in both the bacterial and fungal energy channels. Asynchrony in rates of population turnover among members of the two different energy channels translates into a more stable prey base for the top predators, and thus acts as an important stabilizing mechanism (McCann, 2000; Teng and McCann, 2004) for the soil fauna food web. Thus, soil food webs are considered to be biodiverse, complex, and stable systems (de Castro et al., 2021).

The stability (i.e., the resistance to perturbation) of soil fauna food webs has implications for global processes like climate change that include both long-term changes in temperature and precipitation, as well as greater variability in temperature and precipitation extremes. But the stability of soil fauna communities can be impacted by anthropogenic changes such as both changes in habitat geometry (i.e., the amount, shape, and connectivity of habitat) and disturbance regime (i.e., the spatial and temporal patterns of perturbation). For example, a study of moss-living microarthropods found that species richness and abundance declined corresponding to increased disturbance rate, but that the speed of this decline depended on the connectivity of the surrounding habitat (Starzomski and Srivastava, 2007). In another study, Shackelford et al. (2018) found that microarthropod communities connected to undisturbed landscapes showed a

linear and rapid recovery following a disturbance, whereas those connected to disturbed landscapes showed a hump-shaped recovery and isolated communities showed a slow but linear recovery. However, abiotic factors other than habitat connectivity that may buffer soil fauna communities from disturbances are less well studied.

Stability (resistance, resilience) in soil food webs also depends on food web topology and the dominant microbial energy channel involved. de Vries et al. (2012) found that temperate grassland soil food webs that were dominated by fungi were more resistant, although not resilient, to drought conditions than bacteria-dominated agricultural soil food webs from wheat fields located on the same slope and from the same soil type. Fungal-dominated grassland soil food webs were also found to incorporate C more efficiently, corresponding to lower amounts of C lost through microbial respiration, and fungal-based food webs supported increased diversity and richness of microarthropods. The greater resistance of fungal-dominated soil food webs to perturbation may have been caused by increased resource availability in the form of increased dissolved organic C and fungal biomass, consistent with findings in previous grasslands studies (Cole et al., 2006). In turn, increased microarthropod diversity was associated with increased N leaching from grassland soils (de Vries et al., 2012), consistent with previous findings that microarthropod richness can stimulate N mineralization (Liiri et al., 2002). Overall, these findings suggest that fungal-based soil food webs support a greater evenness of microbial communities and a greater diversity of microarthropods, which in turn helps improve the resistance of soil fauna food webs to the effects of other abiotic factors, like drought (de Vries et al., 2012).

However, the duration and timing of a perturbation can also affect stability outcomes in soil systems. For instance, Thakur et al. (2021) demonstrated that a one-week, ‘pulse’ extreme heat event significantly affected mesocosm soil microbial communities constructed from northern European soils and that differences in microbial community structure between heat shock and ambient treatments were maintained for the duration of the study suggesting low ecosystem resistance and resilience. These findings highlighted the importance of species traits following a disturbance, as the short-term heat event was more detrimental to microbes than microbial predators. Mechanistically, it was suggested that thermal acclimation (e.g., changes in body size or physiological activity) to heat stress promoted predator resilience, but not microbial resilience.

However, it is still unknown how soil fauna food webs will respond to short term disturbances that are expected to become more frequent as a function of climate change (IPCC, 2018). How a soil food web responds to a perturbation with respect to changes in the biomass or metabolism of individual members of the soil food web may subsequently lead to changes in ecosystem-level processes like soil respiration rates (Thompson et al., 2018) ultimately affecting soil C storage potential. However, it is still unknown what effect short-term climate events related to temperature might have on soil fauna food web structure and function, or what role other (potentially mitigating) environmental factors like soil moisture might play. Because C and N cycling are emergent ecosystem properties, resistant and resilient soil communities may better maintain energy and nutrient cycling following a perturbation. This is especially true for disturbance events such as extreme, short-term warming that can alter the metabolic demands of organisms.

1.3 Boreal Peatlands

Boreal peatlands, found across much of northern Canada, are wetlands characterized by low aboveground vascular plant productivity and a thick (in excess of 40 cm deep) layer of peat, or decomposing organic material (Beaulne et al., 2021) arising from slow decomposition. Peatlands are repositories for belowground biodiversity (IUCN, 2021) and are the Earth's largest terrestrial store of soil C (Limpens et al., 2008). Peatlands store C as soil because inputs from aboveground plant productivity exceed the rate at which C is lost from the system through decomposition as heterotrophic respiration (Gorham, 1991). This occurs despite low levels of productivity because rates of decomposition and C cycling through the soil food web are even lower. Low rates of decomposition and heterotrophic respiration occur because of ecostoichiometric limitations like N limitation, resulting from plant inputs that are generally nutrient poor (Bragazza et al., 2006). Nutrient limitations and waterlogged (anoxic) conditions limit the biomasses of soil fauna, which function as secondary decomposers (Xu et al., 2022). Biological activity (e.g., metabolic processes) also occurs at a slow rate because of low soil temperatures (Carrera et al., 2009) and high soil moisture (Bian et al., 2022). Peatland fauna biomasses are often lower than that of forests (IPCC, 2000) or other non-wetland systems, however these systems store a large amount of C because productivity exceeds rates of heterotrophic respiration.

Boreal peatlands are dominated by plants like mosses, sedges, and shrubs (Gore, 1984). In these systems, peat is thereby primarily composed of litter from these plants in varying stages of decomposition. Peat acts to form a pool of biologically available forms of nutrients, like N and phosphorus, to support a complex and species diverse soil food web. At the same time, this peat serves as habitat for complex microbial communities (Asemaninejad et al., 2017, 2019), nematodes (Kamath et al., 2022), and microarthropods (Barreto and Lindo, 2018). Aboveground plant communities are linked to the structure of microbial and faunal communities. For example, microbial communities in moss-dominated systems are characterized by greater ratios of fungi:bacteria, when compared to those in sedge-dominated systems, corresponding to greater plant diversity and lower quality (i.e., high C:N ratio) litter inputs that form peat (Lyons and Lindo, 2020). Correspondingly, the dominant nematode trophic group is related to the dominant microbial group within a system (i.e., fungal-dominated systems contain greater abundance and biomass of fungal-feeding nematodes), and similarly nematode trophic diversity is higher in fungal-dominated peatland food webs than bacterial-dominated food webs (Kamath et al., 2022). Furthermore, nematode communities in nutrient poor, fungal-dominated peatland food webs are more complex than their bacterial-dominated, intermediate nutrient counterparts, due to an increase in the abundance and size of nematode predators (Kamath et al., 2022). While plant litter quality affects the structure of peatland soil food web fungal and bacterial energy channels and is an important driver of decomposition dynamics, abiotic environmental conditions (e.g., temperature, soil moisture) are the main drivers of the structure of microarthropod communities. Specifically, the richness and abundance of microarthropods in boreal peatland hollow microhabitats, characterized by wet depressions, is greater than that observed in hummock microhabitats, characterized by dry and raised areas (Barreto and Lindo, 2018), but at the same time, peatlands with high levels of peat moisture have lower species richness (Barreto and Lindo, 2021). Strong above- and below-ground linkages help reinforce the complexity and stability of peatland soil food webs.

1.4 Effects of Climate Change on Boreal Peatland Soil Food Webs

Climate change involves several environmental changes including increases in ambient temperature, increased variability in temperature, and changes in precipitation that can include

increases, decreases, and increased fluctuations between wet and dry conditions. Global average anthropogenic warming reached +1.25 °C in 2022 (Haustein et al., 2017; Matthews and Wynes, 2022), and the rate of anthropogenic warming is increasing at an estimated 0.2 °C per decade (IPCC, 2018). Changes in temperature are predicted to be more extreme at high latitudes, with short-term extreme warming events (i.e., > 8°C above average) becoming more common (IPCC, 2018). Global precipitation patterns are also anticipated to be highly variable under future climate conditions with many areas experiencing greater than normal wetting or drying of soils (Zhang et al., 2022). In combination with changes in global temperature regimes, changes in precipitation are expected to drive divergent shifts in the hydrology of boreal peatlands. Zhang et al. (2022) found that the 54% of high-latitude peatlands had become dryer over the past 200-years; yet many (32%) high-latitude peatlands had become wetter over this same time period, while several (14%) showed fluctuating hydrological conditions. However, warmer temperatures may indirectly reduce soil moisture content (Holmstrup et al., 2017) through increased evapotranspiration (Seneviratne et al., 2010). It is still unknown whether greater soil moisture may help buffer the effects of temperature through evaporative cooling in the soil microenvironment, or what the combined effects of short-term changes in temperature and soil moisture are on soil food webs and C dynamics.

Both warming and increased peat saturation are anticipated to affect the peatland soil food web and its C transformations. Mechanistically, warming is anticipated to alter decomposer biomass through increasing organismal metabolism that can lead to faster population turnover rates with increased fecundity and death rates (Kuriki, 2008; Li et al., 2019; Pfingstl and Schatz, 2021). Warming also decreases metabolic assimilation and production efficiencies (Luxton, 1972, 1981; Li et al., 2019), potentially reducing population biomasses and therefore reduce trophic transfer of energy and nutrients from one trophic level to the next. Correspondingly, experimental warming has been shown to decrease (Bokhorst et al., 2008) or increase (Lindo, 2015) soil fauna abundances. For instance, Lindo (2015) found increased abundance in smaller bodied invertebrates under warming, while Barreto et al. (2021) found contrasting effects on species richness depending on initial soil moisture conditions of the site. Meehan et al. (2021) found warming increased abundances in soil predators in boreal forests, but whether the soil community was affected by warming was dependent on other (potentially mitigating)

environmental conditions (Meehan et al., 2020). However, it is still unknown what effect short-term extreme climate warming events might have on resistance and resilience of the whole soil food web and C flux, or what role soil moisture might play.

Soil fauna typically show a skewed but unimodal response to soil moisture (Sylvain et al., 2014) where increases in soil moisture are often correlated with increased abundance and species richness of soil microarthropods, except at high levels of soil moisture where reductions in the habitable pore space of soil can reduce soil fauna biomass (Tsiafouli et al., 2005; Turnbull and Lindo, 2015). Alterations in soil moisture can be particularly detrimental for soil organisms in poorly drained, naturally wet soils such as peatlands. For instance, Barreto et al. (2021) found that warming-induced drying of peat soil enhanced faunal species richness where the colonization of more xeric species was possible, but at the expense of peatland-specific semi-aquatic species. The effect of increasing soil moisture on peatland fauna is less well known. Flooded conditions are predicted to become more common with global warming in the 21st century and are predicted to limit soil oxygen availability, thus reducing soil nutrient availability, mineralization, and decomposition of organic material (Schuur and Matson, 2001). Consequently, anaerobic conditions quickly develop in flooded soils (Visser and Voesenek, 2005), which can further cause changes in physical and chemical soil properties (Unger et al., 2010) including the accumulation of phytotoxic products as a function of microbial reduction processes in anoxic conditions (Schuur and Matson, 2001). These changes in soil properties are predicted to affect the composition of soil food webs (González-Macé and Scheu, 2018). However, it is unclear whether the combination of changes in temperature regimes and hydrology expected in peatlands will have an interactive effect on soil food webs, or what effects these changes will have on C and N cycling.

Combined, future warming and changes in soil moisture are thought to threaten the ability of boreal peatlands to sequester C, and may shift boreal peatlands from being a C sink to a C source (Bragazza et al., 2013; Crowther et al., 2016; Harenda et al., 2018). Warming-induced changes in aboveground vegetation (Weltzin et al., 2000; Dieleman et al., 2015; Lyons and Lindo, 2020) and the soil food web (Gilman et al., 2010; Schwarz et al., 2017) drive an increase in total consumptive flux under warming. At the same time, heterotrophic respiration is expected to increase under warming (Brown et al., 2004). Thus, changes in C storage potential for peatland

soil food webs can be examined by calculating the total C flux in the soil food web minus the C lost to the atmosphere as heterotrophic CO_2 respiration. Whether increased soil moisture can buffer the effects of warming on the soil food web and C and N cycling is unknown.

1.5 Research Objectives

My research investigated how a pulse climate warming event affects the peatland soil fauna food web and corresponding C cycling. My overall objective was to determine how extreme heat and changes in hydrology affect the resistance and resilience of a peatland soil food web and its C functions. Specific objectives included:

1. Comparing the abundances of the microfauna (nematodes) and mesofauna (microarthropods), and microbial activity (enzyme activity) under short-term (i.e. 21-days), extreme climate perturbations of temperature and soil moisture relative to a field-based control conditions using peat mesocosms and a full-factorial design (Resistance).
2. Examining whether any measurable response of perturbed mesocosms is mitigated when mesocosms are returned to field-based temperatures (Resilience).
3. Modeling the C and N flux and mineralization through the soil fauna food web immediately following short-term, extreme climate perturbations of temperature and soil moisture and following a recovery period using an energetic food web model.

I hypothesized that warming will accelerate reproductive rates, especially in small-bodied organisms. Thus, I predicted that soil fauna abundances would increase under warming. At the same time, I hypothesized that greater soil moisture would reduce total soil fauna abundances, corresponding to a reduction in total habitable pore spaces in saturated soils. Correspondingly, I predicted that average total biomass will be greatest in mesocosms assigned to +8 °C warming and field-moist conditions and will be least in those assigned to ambient temperature and saturated conditions. I also hypothesized that soil moisture will enhance system resistance and resilience to heat shock due to the specific heat capacity of water. Thus, I predicted that biomasses in mesocosms assigned to +8 °C warming and saturated conditions will be more resistant and resilient than those assigned to +8 °C warming and field-moist conditions. Furthermore, I predicted that biomasses in mesocosms assigned to +8 °C warming and saturated

conditions would be more similar between sampling times immediately following (T_1) the climate perturbation and after a recover period (T_2) than those assigned to +8 °C warming and field-moist conditions.

In the energetic model of the system, I predicted that the total C flux and C mineralization through the soil fauna food web will be directly correlated with soil fauna population biomasses and temperature-mediated metabolism. Thus, I predicted that C flux and C mineralization will be greatest under +8 °C warming and field-moist conditions and least under ambient temperature and saturated conditions while exposed to the temperature/moisture perturbation. At the same time, I predict that when temperature-mediated metabolic demands are removed, differences between temperature treatments will be more similar, but biomass shifts resulting from alterations in soil moisture will persist as these conditions will take longer to recover from.

I used a paired empirical and model approach to capture changes in both the soil community and larger ecosystem functioning under warming and hydrological changes. Comparing empirical changes in abundance and biomass allowed me to examine population level responses in the soil food web at the level of individual nodes, but this approach alone is limited in generalizability as it does not capture emergent soil properties that operate at the scale of whole ecosystems and landscapes. Integrating both empirical and model approaches will allow me to better understand how changes in ecosystem level functions like soil C and N transformations emerge from changes at the level of individual nodes in the soil fauna food web.

Chapter 2

2 Methods and Experimental Design

2.1 Soil Sampling

Peatland soils were collected in September 2021 from a *Sphagnum*-dominated peatland that is part of the BRACE (Biological Response to A Changing Environment) experimental peatland project in the southern boreal mixed-wood forest ecozone. This site is located near White River, Ontario, Canada (48°21′ N, 84°20′ W), and is a long-term research monitoring site used by the Ontario Ministry of Natural Resources and Forestry for the past 20 years. The peatland is a nutrient-poor fen, with a pH ~4.1 and a water table ~30 cm deep that fluctuates seasonally. Previous studies at this site have characterized vegetation (Lyons and Lindo, 2020), bacterial and fungal communities (Asemaninejad et al., 2017, 2019), nematodes (Kamath et al., 2022), and soil microarthropods (Barreto et al., 2021).

Intact peat core samples (8 × 8 cm × 15 cm deep) were cut and removed using a small, hand peat saw from randomly selected 'lawn' areas (i.e., avoiding hummocks and hollows) that were dominated by *Sphagnum* spp. to exclude vascular plants as much as possible. To account for any heterogeneity in the sampling location, samples were collected in blocks that represented nearby locations of lawn areas, but all samples were collected within a roughly 25 m × 25 m area. Some sample locations were characterized by high microfauna and high mesofauna abundance and were subsequently dealt with in the statistical analyses using block effects (i.e., two blocks, high and low abundance). Intact peat cores were placed in individual plastic bags, kept cool in the field, and refrigerated (4 °C) until the start of the experiment within 48 hours of sample collection. A total of 45 peat core samples were collected.

In the lab, each intact peat core was placed into a 500 mL glass jar to create experimental mesocosms that were placed into incubation at 12 °C under field moist conditions for two weeks to allow each mesocosm to recover from the disturbance. Both the weight of the soil core and the final weight of the mesocosm (soil plus jar) was recorded to monitor moisture loss and replace moisture loss as necessary during the experiment. Following this recovery period, five mesocosms were selected to be destructively sampled (T_0). The remaining 40 mesocosms were

randomized into experimental treatments of temperature (12 °C and 20 °C) and moisture level regime (field-moist and saturated soil moisture) with ten replicates of each factorial treatment (12 °C field-moist, 12 °C saturated, 20 °C field-moist, 20 °C saturated). Temperature treatments were chosen to reflect the average ambient growing season temperature of the area (12 °C) and an extreme warming event of +8 °C. The southern boreal zone is predicted to see ~4 °C increases in mean annual surface temperature by the end of the century, with increased occurrence of 'heat waves' (Perkins-Kirkpatrick and Lewis, 2020), while increases of ~8 °C in mean annual surface temperature are forecast for northern boreal and subarctic areas (Price et al., 2013). Air temperature data from the field site over the past four years indicate that peat-soil surface air temperatures reach or exceed 30 °C at least two days per year, and average soil surface temperatures exceed 20 °C for prolonged periods during summers. Soil moisture regimes were chosen to represent one possible water table scenario that future peatlands may experience under climate change, which has potential for both drying and wetting conditions as well as fluctuations between the two (Zhang et al., 2022).

Mesocosms were placed under experimental treatment for three weeks, before five replicates of each factorial treatment were destructively sampled (T_1). Moisture content across all mesocosms was maintained by adding water to replace any moisture lost during three weeks of experimental conditions. The 20 remaining mesocosms were returned to ambient incubation temperatures for an additional three weeks before they were destructively sampled (T_2). At the same time, moisture was no longer added to mesocosms assigned to saturated conditions so that these mesocosms were allowed to slowly return to ambient moisture conditions but moisture in field-moist samples was maintained as described. The T_1 mesocosms represent the immediate soil food web response to incubation climate conditions under each assigned combination of temperature and moisture level (resistance to perturbation), while mesocosms sampled at T_2 represent mesocosms from each experimental treatment group following three weeks of recovery under ambient temperatures and a slow return to field-moist conditions (resilience).

2.2 Mesocosm Sampling

Each week during the experiment, mesocosms were assessed for soil heterotrophic respiration. These carbon losses, as CO_2, were measured every 7 days during the experiment from each

mesocosm using a Licor Infrared Gas Analyser (IRGA) with a multiplexing system. Briefly, each mesocosm was sealed, air-filled headspace was purged from the mesocosm, and CO_2 concentration was measured every 2 sec over a 90 sec period. Soil heterotrophic respiration was recorded in the units μMol CO_2 per m^2 per s and converted to g of C per m^2 per year. Heterotrophic respiration was measured for all mesocosms at T_0. For the T_1 mesocosms, heterotrophic respiration was calculated as the average measurement across the four weeks (i.e., starting from the beginning of the experiment (T_0) and ending with the destructive sampling of T_1 mesocosms three weeks later). The T_2 mesocosms are calculated as the average across three weeks of recovery time.

Mesocosms were destructively sampled according to assigned destructive sampling treatments. Accordingly, destructive sampling was performed at three time points: T_0 (pre-experiment), T_1 (resistance to perturbation), and T_2 (resilience following recovery). Destructive sampling included soil fauna extractions to assess the soil food web for soil microfauna (nematodes) and soil microarthropods (mites and collembola), and enzyme assays for microbial potential activity. For each mesocosm, approx. 20 g wet weight of peat was extracted for nematodes and approx. 50 g wet weight peat was used for extraction of microarthropods. Wet extractions (Baermann funnel technique e.g., Forge and Kimpinski, 2008) over 48 hours were used to collect nematodes in water from each mesocosm. Nematodes were preserved in 4% formalin and Rose Bengal stain and enumerated under a stereomicroscope; biomass estimates for fungivores, bacterivores, omnivores, and predators were calculated based on previously established relative abundance distributions and individual body size measurements for each trophic group at the research site (Kamath et al., 2022) and allometric equations of Andrássey (1956). Microarthropods were dry extracted using Tullgren funnels over 72 hours into 75% EtOH, and identified at the suborder-to-family level into the following trophic groups under a stereomicroscope: collembola, juvenile oribatid mites, adult oribatid mites, other non-predatory mites (i.e., most Prostigmata and Astigmata), nematode feeding mites (i.e., Zerconiidae), arthropod feeding mites (i.e., most Mestostigmata excluding Zerconiidae). Oribatid mites were separated into adults vs. juveniles to account for differences in sclerotization that could affect predation rates (see Peschel et al., 2006). Microarthropod abundances were converted to biomass using established allometric equations based on body size (e.g., Edwards, 1967 for collembola; Lebrun, 1971 for oribatid,

prostigmatid, and astigmatid mites; Persson and Lohm, 1977 for mesostigmatid mites). All abundances (nematodes and microarthropods) were standardized by the final dry weight of peat soil used in the extraction.

During the process of destructive sampling, mesocosms were also assessed for physical soil properties and enzyme activity. Soil moisture and pH were measured on 5 g subsamples of each mesocosm using standard soil methods (i.e., gravimetrically and in water, respectively), while percent total C and N were analysed on a CNSH analyser (Elementar Americas IsoCube, New York, USA). A soil enzyme assay protocol modified from Saiya-Cork et al. (2002) was used to measure phenol oxidase and peroxidase activity on 1 g subsamples of each mesocosm.

2.3 Mesocosm Experiment Empirical Analysis

To compare soil communities under varying temperature and soil moisture conditions, I first analyzed empirical data generated during the mesocosm experiment. One sample (#5) was excluded from all analyses due to an extremely high abundance of both micro- and meso-fauna, including disk-shaped astigmatic mites that were uncommon in all other samples. Heterotrophic respiration was tested for normality and homogeneity of variance using a Shapiro-Wilk test with Q-Q plot and Levene's test with residuals vs. fit plot, respectively. Mean heterotrophic respiration was compared across each combination of soil moisture, temperature, and destructive sampling conditions using a three-way full-factorial ANOVA with a block effect to account for differences in total abundance by original sampling location with high biomass values of both microfauna and mesofauna observed in a single block that contained one sample replicate from each treatment and Tukey's HSD post-hoc test.

Soil properties and enzyme concentrations were tested for normality and homogeneity of variance using a Shapiro-Wilk test and Levene's test, respectively. I constructed linear models from soil properties and enzyme activity using reverse order selection to remove insignificant interaction terms (see Appendix F). Soil properties and enzyme activities were then compared across combinations of soil moisture, temperature, and destructive sampling conditions using a three-way ANOVA with a block effect and Tukey's HSD post-hoc test.

Microfauna, mesofauna, and total faunal abundance (standardized abundance by dry weight) were tested for normality and homogeneity of variance using a Shapiro-Wilk test with Q-Q plot and Levene's test with residuals vs. fit plot, respectively. I used Pearson's correlation test to examine correlations between soil microfauna, mesofauna, and total faunal abundances. I constructed linear models from total abundance, soil microfauna abundance, and soil mesofauna abundance using reverse order selection to remove insignificant interaction terms (see Appendix F). I then statistically analysed differences in total microfauna, total mesofauna and total faunal abundance between treatments at T_1 and T_2 using a three-way full-factorial ANOVA with a block effect to account for any field-based differences in abundance. I similarly used a full-factorial ANOVA with a block effect and Tukey's HSD post-hoc test to test for differences in biomass and average weekly soil heterotrophic respiration between treatments. To assess resistance of the system I compared the mean total and trophic group abundance and enzyme concentrations within each treatment group relative to T_1. The resilience of the system was assessed by determining whether changes in total and trophic group abundance and enzyme concentrations observed at T_1 were maintained at T_2.

To examine whether the overall soil fauna (microfauna and mesofauna) groups significantly changed following experimental treatments (T_1) and remained different following the recovery period (T_2), I performed a multivariate PerMANOVA (permutational ANOVA) based on Bray Curtis dissimilarity of soil fauna trophic groups using the vegdist function to create the dissimilarity matrix, the adonis2 function for the PerMANOVA, and visually display the data using non-metric multidimensional scaling (NMDS) in the R package *vegan* (Oksanen et al., 2020).

2.4 Energetic Food Web Modelling and Statistical Analysis

To compare ecosystem function under varying temperature and soil moisture conditions, I modelled C and N fluxes and mineralization (see Figure 1.1) using food webs (see Figure 2.1) constructed from node biomasses generated during the mesocosm experiment. Energetic food web models (*sensu* Moore and de Ruiter, 2012) use three matrices of data to calculate an estimate flux of C and N through the food web: 1) information about death rates and feeding efficiencies for each node based on established values from the literature (see Appendix A), 2) a

matrix of feeding relationships (links; see Appendix B), and 3) biomass values for each food web member (nodes; see Appendix C). Population turnover rates (death rates) (*d*) and trophic (production) efficiencies (E_p) were scaled to account for temperature-mediated changes in metabolic rate (Brown et al., 2004) in the 20 °C mesocosms (see Appendix A).

The basal food web nodes included basal resources consisting of (1) labile and (2) recalcitrant detritus estimated based on previously measured soil organic C quality measurements and litter input rates (Webster et al., 2013; Palozzi and Lindo, 2017). It is important to note that in the model the biomass of the basal resource was always in excess. The microbial groups included (3) bacteria, (4) fungi, and (5) protists that were previously assessed at this site using phospholipid fatty acid (PLFA) analysis (Lyons and Lindo, 2020). I quantified the biomass of the remaining soil food web nodes as described above for (6) bacterivorous nematodes, (7) fungivorous nematodes, (8) omnivorous nematodes, (9) predatory nematodes, (10) collembola, (11) adult oribatid mites, (12) juvenile oribatid mites, (13) non-predatory prostigmatid and astigmatid mites, (14) nematode-feeding mites (Mesostigmata: Zerconiidae), and (15) arthropod feeding mites (remaining Mesostigmata) (Figure 2.1). Biomass estimates based on empirical data were generated for 15 soil food web nodes to form the basis of the energetic food web model (see Figure 2.1 for placement of each trophic node in the food web). All biomass values are g C / m^2 / year for all nodes.

Total C and N flux values were estimated for the entire food web of each mesocosm (T_0, T_1 and T_2) using the R package *soilfoodwebs* (Buchkowski et al., 2023). I also estimated total C and N fluxes in the fungal and bacterial energy channels corresponding to each mesocosm (see Figure 2.1). The *soilfoodwebs* package is an ecostoichiometric model that calculates fluxes of C and N through the food web assuming equilibrium (Buchkowski and Lindo, 2021). Flux values of N are calculated using data on the C:N ratio of each organism (Appendix A). Total flux is the amount of C and N transferred via consumption across food web members and is also partitioned into the amount C and N mineralized (for C this is respiration) vs. C and N retained in the food web as biomass.

Total biomass, microfauna biomass, mesofauna biomass, total flux, total C mineralization, and N mineralization were tested for normality and homogeneity of variance using a Shapiro-Wilk test

and Levene's test, respectively. I constructed linear models from total biomass, microfauna biomass, mesofauna biomass, total flux, total C mineralization, and total N mineralization using reverse order selection to remove insignificant interaction terms (see Appendix F). I then statistically analyzed the biomasses of total microfauna, total mesofauna and total faunal between each combination of soil moisture, temperature, and destructive sampling conditions using a three-way full-factorial ANOVA with a block effect to account for any field-based differences in biomass and Tukey's HSD post-hoc test. I similarly analyzed the output C and N flux and mineralization values of the whole soil food web model using a 3-way factorial ANOVA and Tukey's HSD post-hoc test to examine differences between soil moisture, temperature, and destructive sampling treatment conditions. Finally, I used Pearson's correlation test to test for correlations between soil microfauna, mesofauna, and total faunal biomasses.

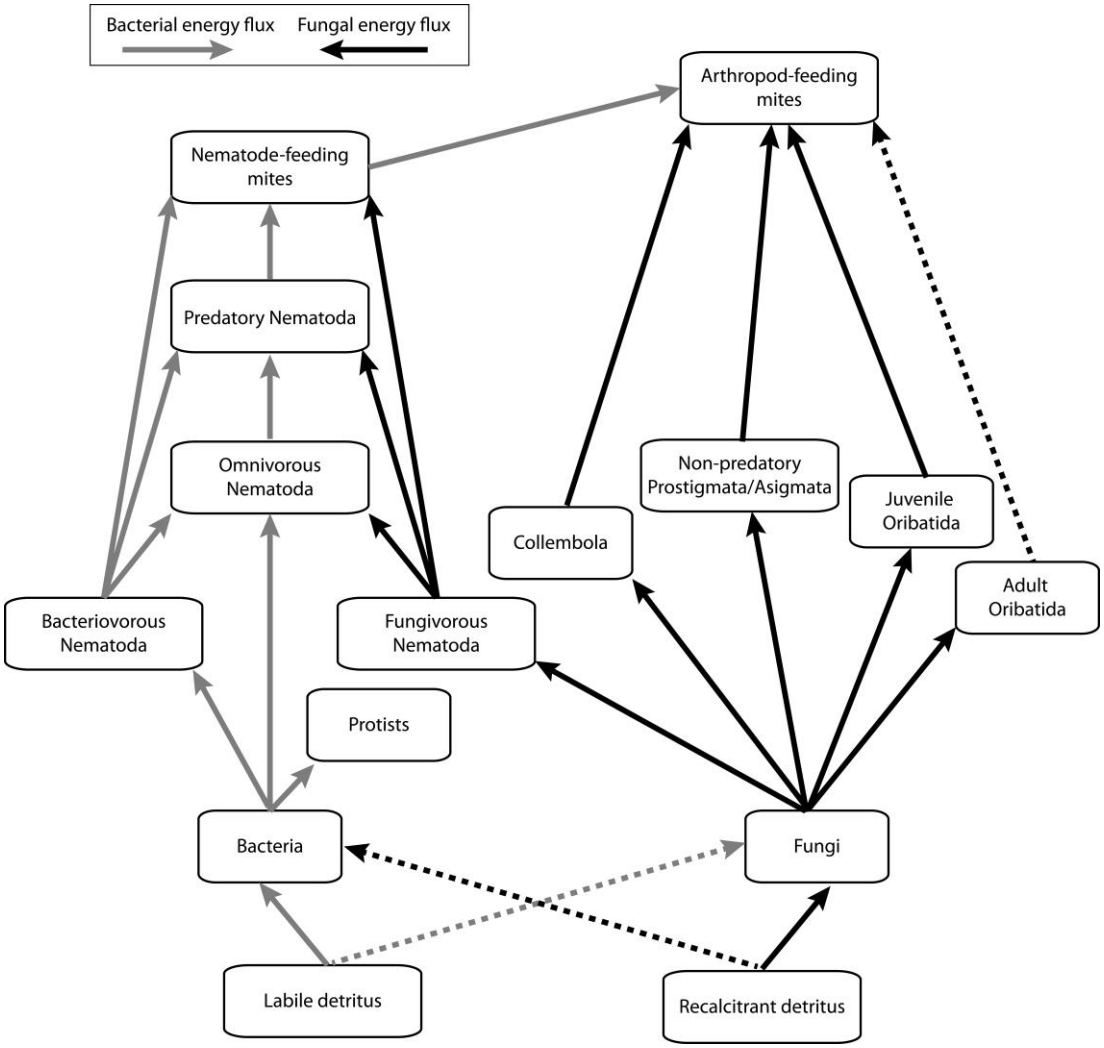

Figure 2.1 The conceptualized peatland soil food web containing 15 trophic nodes (groups).

Arrows represent the flow of energy (carbon) and nutrients corresponding to trophic interactions from resources to consumers. Nodes, shown as boxes, represent distinct phylogenetic groups of soil fauna, microflora and detritus. Dashed lines represent weaker trophic interactions. Grey arrows are bacterial energy channel; black arrows are fungal energy channel.

Chapter 3

3 Results

3.1 Pre-experimental Group (T_0)

Five experimental mesocosms were destructively sampled following a three-week recovery period but prior to deployment of the experimental treatments (T_0). The following conditions were recorded for these five control mesocosms and were assumed to be representative of field values. The mean heterotrophic respiration (± SE) prior to implementing experimental soil moisture and temperature conditions at T_0 was 7.0 ± 0.2 ln(g of C per m^2 per year), which equates to ~1200 ± 200 g of C per m^2 per year. The mean soil moisture (± SE) was 830 ± 110% based on a dry weight gravimetric measurement, while the average soil pH (± SE) was 4.08 ± 0.05. Mean C:N ratio (± SE) was 37 ± 2, while mean microbial enzymatic activity (± SE) was 160 ± 16 μmol substrate per g soil per hour for phenol oxidase and 154 ± 8 μmol substrate per g soil per hour for peroxidase concentration. The mean total microfauna, mesofauna, and total fauna abundances (± SE) were: 170,000 (± 40,000), 360,000 (± 40,000), and 540,000 (± 50,000) individuals per m^2, respectively.

Converting faunal abundance to biomass estimates, I calculated a mean microfauna, mesofauna and total fauna biomass (± SE) as 0.009 (± 0.002), 0.73 (± 0.08), and 0.74 (± 0.08) g of C per m^2, respectively. Mean total consumptive flux (± SE) based on the energetic model was 1261 ± 4 g of C per m^2 per year, while the mean total C mineralization (± SE) was 514 ± 2 g of C per m^2 per year, and the mean total N mineralization (± SE) was -4.51 ± 0.02 g of N per m^2 per year. Mean values are presented in Appendix D.

3.2 Soil Heterotrophic Respiration

Heterotrophic respiration was transformed on natural log, (ln) scale to conform to the assumption of normality. Log-transformed soil heterotrophic respiration satisfied the assumptions of normality and homodescacity, as per a Shapiro-Wilk ($W = 0.983$, $p = 0.799$) and Levene's test ($F_{7,31} = 0.555$, $p = 0.786$). Log-transformed heterotrophic respiration, estimated for each mesocosm (Figure 3.1), was not significantly affected by soil moisture ($F_{1,34} = 1.670$, $p = 0.205$),

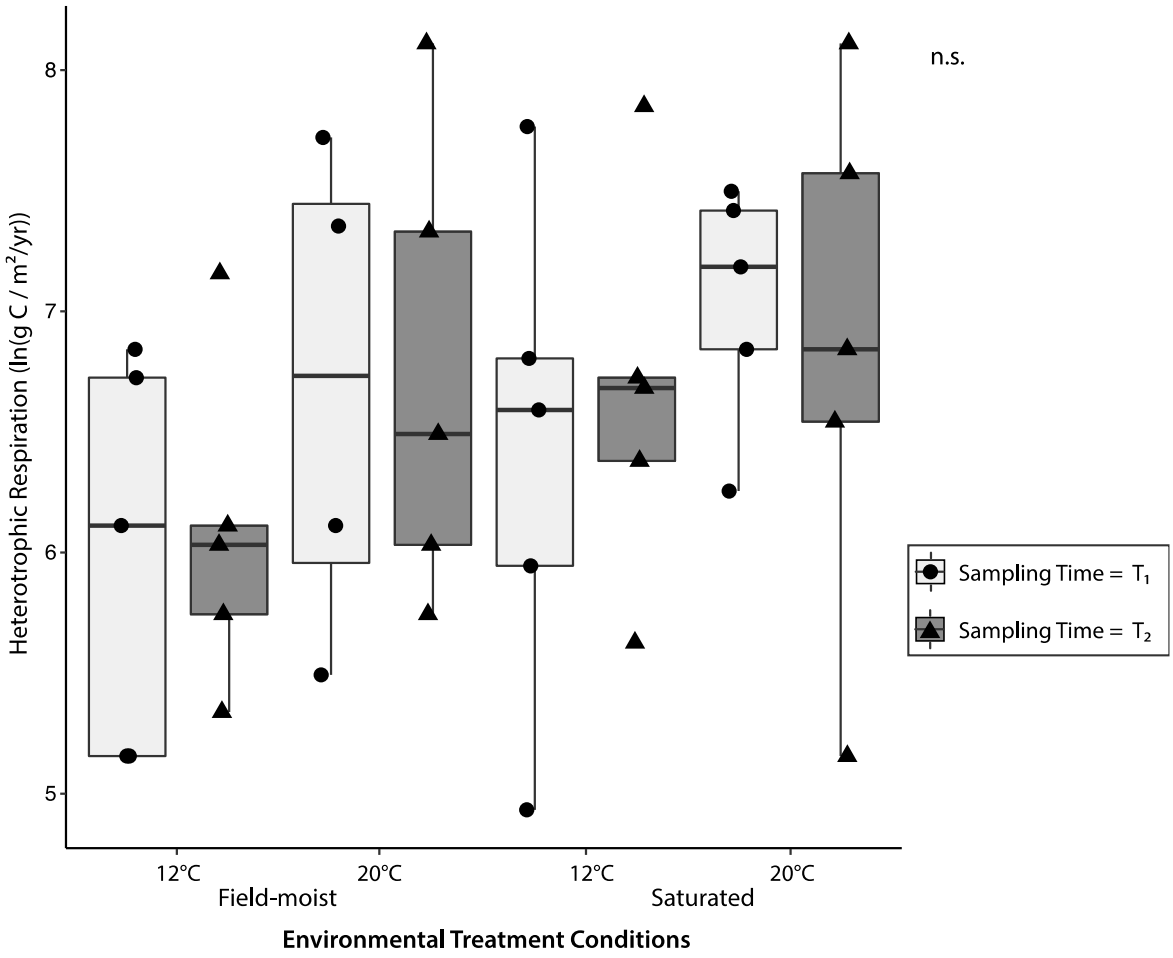

Figure 3.1 Boxplots of mean heterotrophic soil respiration (ln transformed).

Measurements were taken during the three-week experimental climate disturbance scenarios (T_1) under each combination of temperature (12 °C, 20 °C) and soil moisture (field-moist, saturated) treatments, and during the following three-week recovery period (T_2) when mesocosms were returned to in field conditions (12 °C, field-moist).

but was significantly affected by temperature ($F_{1,34}$ = 3.975, p = 0.054); heterotrophic respiration was greater in mesocosms assigned to 20 °C vs. 12 °C. Neither destructive sampling time ($F_{1,34}$ = 0.109, p = 0.743) nor block effects ($F_{1,34}$ = 0.243, p = 0.6125) used to account for differences in field sampling location significantly affected log-transformed respiration. There were no significant interaction effects between soil moisture, temperature, and destructive sampling time (Appendix E). Mean soil heterotrophic respiration (± SE) under each treatment is presented in Appendix D. Estimates of effect size based on a linear model are given in Appendix F.

3.3 Physical Soil Properties

Soil moisture and pH were transformed on natural log, (ln) scale to conform to the assumption of normality. Soil moisture and pH were measured across 37 experimental mesocosms; in addition to sample ExRes 5, one large positive outlier (point estimates: 7.10 ln(%), 1.55 ln(pH)) and one large negative outlier (point estimates: 6.34 ln(%), 1.28 ln(pH)) were removed to help conform to the assumptions of normality. Soil C:N ratio was compared across 36 mesocosms, as three samples could not be processed due to the mass and packing of the sample and size limitations of the CNSH autosampler. Log-transformed soil moisture (Shapiro-Wilk's test: W = 0.942, p = 0.055; Levene's test: $F_{7,29}$ = 0.165, p = 0.990), log-transformed pH (Shapiro-Wilk's test: W = 0.976, p = 0.596; Levene's test: $F_{7,29}$ = 0.929, p = 0.499), and C:N ratio (Shapiro-Wilk's test: W = 0.985, p = 0.897; Levene's test: $F_{7,28}$ = 1.090, p = 0.398) each satisfied the assumptions of normality and homogeneity of variance.

Mean soil moisture (Figure 3.2A) was significantly related to the induced soil moisture treatments and significantly greater in saturated vs. field-moist treatments ($F_{1,32}$ = 18.407, p < 0.001), but was not influenced by temperature treatments ($F_{1,32}$ = 1.856, p = 0.183). Soil moisture was not affected by destructive sampling time ($F_{1,32}$ = 0.695, p = 0.411) nor block effects ($F_{1,32}$ = 0.159, p = 0.693). There were no significant interaction effects between soil moisture, temperature, and destructive sampling time (Appendix E). Mean soil moisture is presented in Appendix D. Estimates of effect size based on a linear model are given in Appendix F.

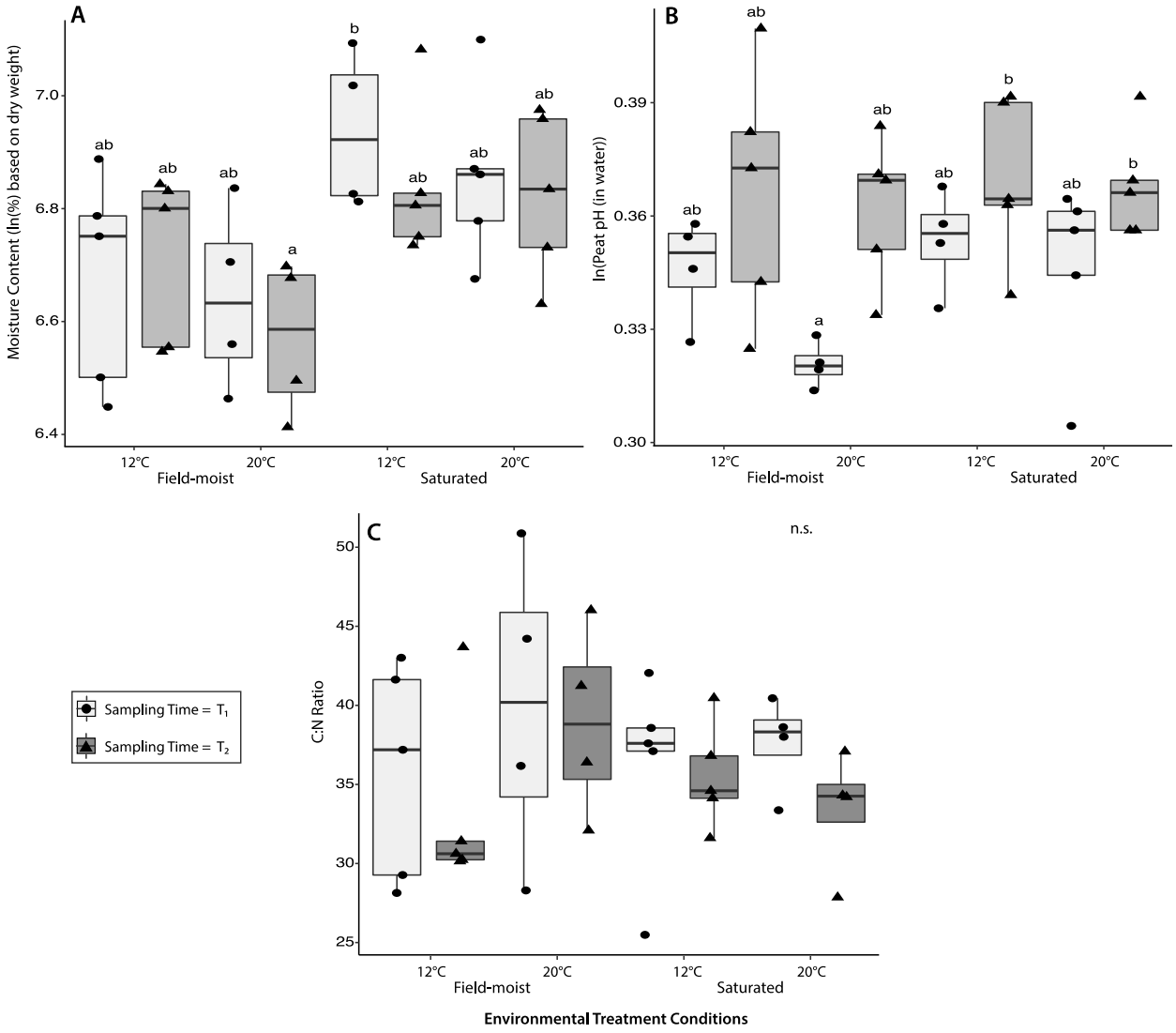

Figure 3.2 Soil moisture (A), pH (B), and C:N ratio (C).

Mesocosms were measured across experimental treatments of temperature (12 °C, 20 °C) and soil moisture (field-moist, saturated) destructively sampled after three-weeks (T_1) or following three-week recovery period (T_2). Letters denote significant differences between groups, as per Tukey's HSD test.

Mean soil pH (Figure 3.2B) was not significantly influenced by soil moisture ($F_{1,32} = 2.097$, $p = 0.157$) nor temperature ($F_{1,32} = 1.630$, $p = 0.211$) treatments. Destructive sampling time exhibited a significant effect on pH ($F_{1,32} = 12.166$, $p = 0.001$) and pH tended to be greater in mesocosms sampled at T_2 vs. T_1, but block effects did not explain differences in pH between treatments ($F_{1,32} = 0.028$, $p = 0.868$). There were no significant interaction effects between soil moisture, temperature, and destructive sampling time (Appendix E). Mean soil pH is presented in Appendix D. Estimates of effect size based on a linear model are given in Appendix F.

Soil C:N (Figure 3.2C) did not show any clear trends across treatments. Neither soil moisture ($F_{1,31} = 0.398$, $p = 0.533$), temperature ($F_{1,31} = 1.522$, $p = 0.227$), nor destructive sampling time ($F_{1,31} = 0.502$, $p = 0.484$) had a significant effect on soil C:N ratio. There was no significant difference in C:N ratio between treatments corresponding to block effects ($F_{1,31} = 1.038$, $p = 0.316$) and there were no significant interaction effects between soil moisture, temperature, and destructive sampling time (Appendix E). Mean C:N (± SE) under each treatment is presented in Appendix D. Estimates of effect size based on a linear model are given in Appendix F.

3.4 Enzyme Activity

Mean phenol oxidase activity was measured across 38 mesocosms. One anomalous negative reading indicating an issue with instrumental background noise was excluded from both phenol oxidase and peroxidase comparisons. Peroxidase activity was compared across 37 mesocosms, as one large positive outlier (point estimate = 323 μmol substrate per g soil per hour) was additionally omitted. Mean phenol oxidase (Shapiro-Wilk: $W = 0.959$, $p = 0.182$; Levene: $F_{7,30} = 2.100$, $p = 0.075$) and peroxidase (Shapiro-Wilk: $W = 0.946$, $p = 0.074$; Levene: $F_{7,29} = 0.584$, $p = 0.763$) activity satisfied the assumptions of normality and homogeneity of variance, as per a Shapiro-Wilk test and Levene's test, respectively.

Mean phenol oxidase activity (Figure 3.3A) was not significantly affected by soil moisture treatments ($F_{1,32} = 0.760$, $p = 0.390$), but was strongly driven by temperature conditions ($F_{1,32} = 16.455$, $p < 0.001$). Mean phenol oxidase activity increased in mesocosms assigned to 20 °C vs. 12 °C conditions. Destructive sampling treatments also significantly affected phenol oxidase

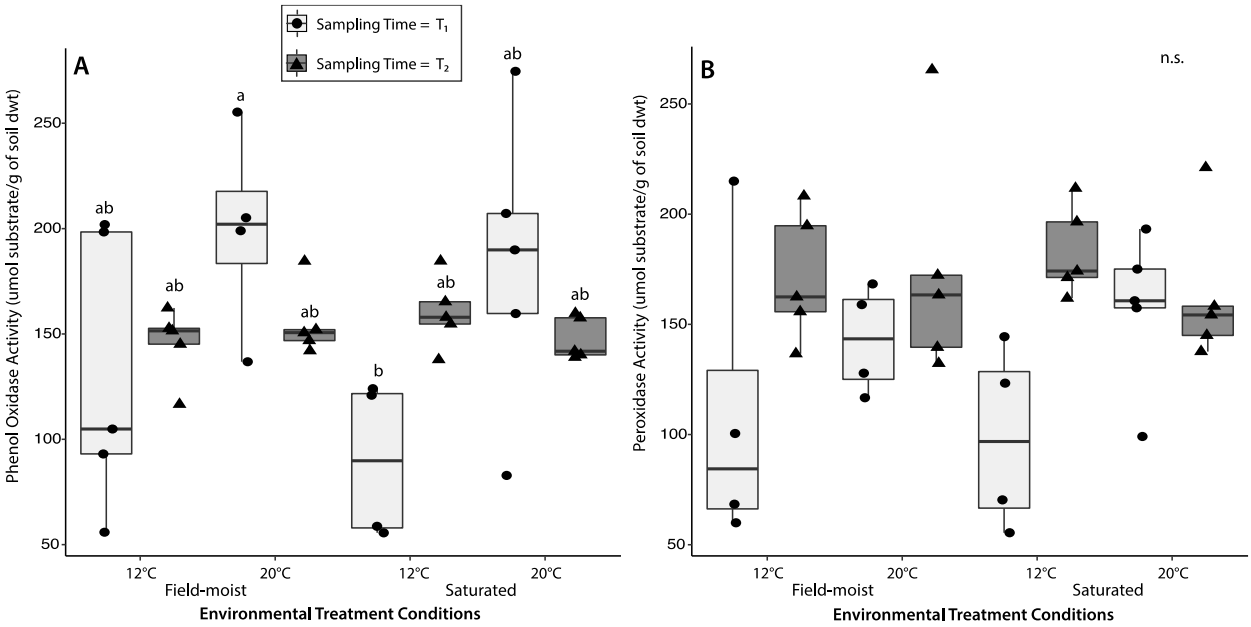

Figure 3.3 Boxplots of mean phenol oxidase (A) and peroxidase (B) concentration.

Measurements were taken across experimental treatments of temperature (12 °C, 20 °C) and soil moisture (field-moist, saturated) destructively sampled after three-weeks (T_1) or following three-week recovery period (T_2). Letters denote significant differences between groups, as per Tukey's HSD test.

activity ($F_{1,32}$ = 0.581, p = 0.452) and was greater at T_2 vs. T_1. This was driven by a significant temperature by destructive sampling time interaction ($F_{1,32}$ = 9.001, p = 0.005), which suggests that phenol oxidase activity decreased in mesocosms assigned to 20 °C from T_1 to T_2 following a three-week return to initial 12 °C conditions. Block effects constructed corresponding to differences in total abundance by original sampling location ($F_{1,32}$ = 1.159, p = 0.290) did not have a significant effect on phenol oxidase activity. There were no other significant interaction effects between soil moisture, temperature, and destructive sampling time (Appendix E). Overall, mean phenol oxidase activity (± SE) was greatest (199 ± 24 μmol substrate per g soil per hour) in mesocosms assigned to 20 °C field-moist conditions, sampled at T_1 and was least (90 ± 19 μmol substrate per g soil per hour) in those assigned to 12 °C saturated conditions, sampled at T_1 (see Appendix D). Estimates of effect size based on a linear model are given in Appendix F.

Mean peroxidase activity (Figure 3.3B) was not influenced by soil moisture ($F_{1,31}$ = 0.009, p = 0.925), but was significantly affected by temperature ($F_{1,31}$ = 6.955, p = 0.013) and increased at 20 °C vs 12 °C. Mean peroxidase activity was also significantly affected by destructive sampling treatments ($F_{1,31}$ = 20.949, p < 0.001) and was greater in mesocosms sampled at T_2 vs. T_1. This was driven by a significant temperature by destructive sampling time interaction ($F_{1,31}$ = 5.235, p = 0.029), which suggests that peroxidase activity also decreased in mesocosms assigned to 20 °C from T_1 to T_2 following a three-week return to initial 12 °C conditions. Block effects also significantly influenced mean peroxidase activity ($F_{1,31}$ = 6.091, p = 0.019); peroxidase activity tended to decrease in blocks characterized by especially high soil fauna abundances. There were no other significant interaction effects between soil moisture, temperature, and destructive sampling time (Appendix E). Mean peroxidase concentration (± SE) under each treatment is presented in Appendix D. Estimates of effect size based on a linear model are given in Appendix F.

3.5 Soil Fauna Abundance and Biomass

Mean total soil fauna abundance (Shapiro-Wilk's test: W = 0.980, p = 0.701; Levene's test: $F_{7,31}$ = 0.435, p = 0.872) and total soil microfauna abundance (Shapiro-Wilk's test: W = 0.980, p = 0.704; Levene's test: $F_{7,31}$ = 0.955, p = 0.480) each satisfied the assumptions of normality and homogeneity of variance, as per a Shapiro-Wilk's test and Levene's test. Total soil mesofauna

abundance was transformed on natural log, (ln) scale to conform to the assumption of normality (Shapiro-Wilk's test: $W = 0.976$, $p = 0.564$; Levene's test: $F_{7,31} = 0.389$, $p = 0.901$). Total biomass (Shapiro-Wilk's test: $W = 0.953$, $p = 0.107$; Levene's test: $F_{7,31} = 0.317$, $p = 0.940$), total soil microfauna biomass (Shapiro-Wilk's test: $W = 0.980$, $p = 0.704$; Levene's test: $F_{7,31} = 0.955$, $p = 0.480$), and total soil mesofauna biomass (Shapiro-Wilk's test: $W = 0.953$, $p = 0.105$; Levene's test: $F_{7,31} = 0.313$, $p = 0.943$) each met the assumptions of normality and homogeneity of variance.

Total soil microfauna and mesofauna abundances were significantly correlated ($R_{42} = 0.467$, $p = 0.001$); similarly, soil microfauna ($R_{42} = 0.834$, $p < 0.001$) and mesofauna ($R_{42} = 0.877$, $p < 0.001$) total abundances were each significantly and positively correlated with total fauna abundance. Mean total soil fauna abundance (Figure 3.4A) was strongly influenced by the original sampling location (i.e., significant block effects ($F_{1,34} = 22.953$, $p < 0.001$)) with a high abundance of both microfauna and mesofauna observed in a single block that contained one sample replicate from each treatment. Total abundance of soil fauna was significantly reduced under saturated vs. field-moist conditions ($F_{1,34} = 19.104$, $p < 0.001$). This was driven by decreased microfauna ($F_{1,34} = 21.152$, $p < 0.001$) and mesofauna ($F_{1,33} = 6.143$, $p = 0.018$) abundances. Destructive sampling did not affect total fauna abundance ($F_{1,34} = 0.466$, $p = 0.499$), soil microfauna abundance ($F_{1,34} = 0.966$, $p = 0.33$), nor soil mesofauna abundance ($F_{1,33} = 1.968$, $p = 0.170$). Neither total soil fauna abundance nor soil microfauna abundance was significantly affected by interaction effects (Appendix E), but soil mesofauna exhibited a significant temperature by destructive sampling time interaction effect ($F_{1,33} = 4.276$, $p = 0.047$). This suggests that soil mesofauna abundances in mesocosms assigned to 20 °C decreased from T_1 to T_2 following a three-week return to initial 12 °C conditions. Overall, mean total abundance (± SE) was greatest (360,000 ± 70,000 individuals per m^2) in mesocosms assigned to 20 °C field-moist conditions, sampled at T_1 and was lowest (150,000 ± 30,000 individuals per m^2) in those assigned to 12 °C saturated conditions, sampled at T_1 (see Appendix D). Estimates of effect size based on a linear model are given in Appendix F.

Following trends in soil fauna abundance, total soil microfauna and mesofauna biomasses were significantly correlated ($R_{42} = 0.460$, $p = 0.002$) as was total soil microfauna ($R_{42} = 0.478$, $p = 0.001$) and mesofauna ($R_{42} = 0.999$, $p < 0.001$) biomasses with total faunal biomass. Mean total

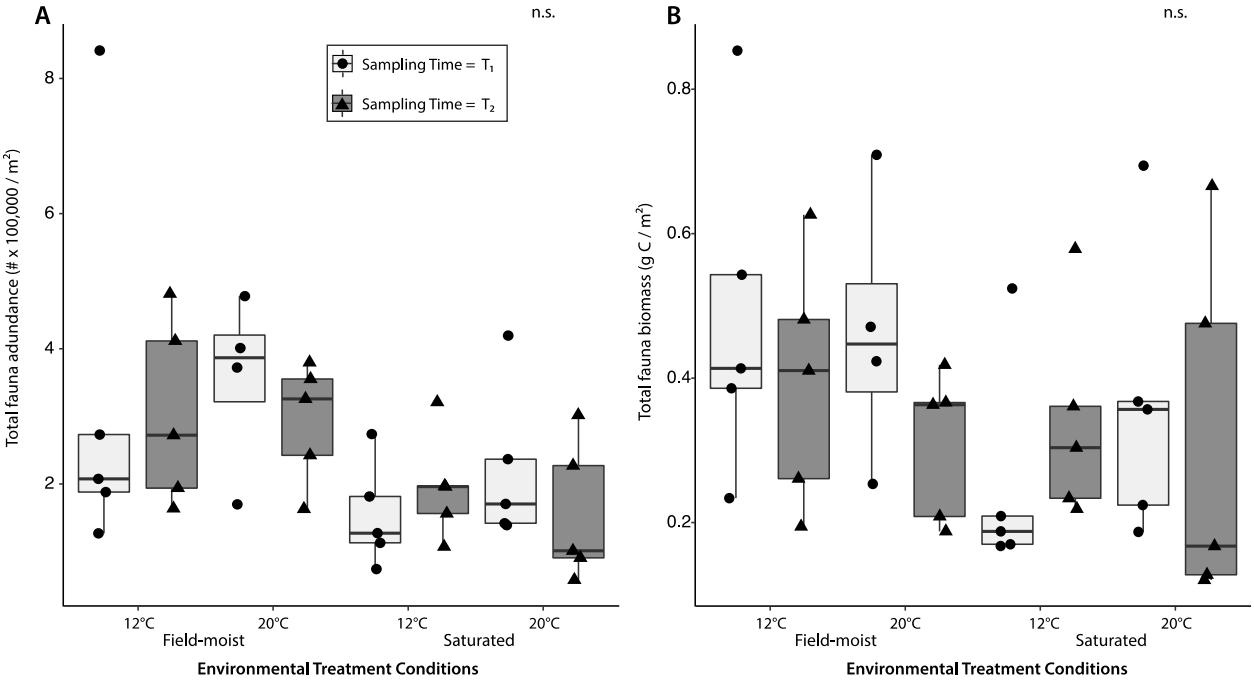

Figure 3.4 Boxplots of mean fauna abundance (A) and biomass (B).

Mesocosms were assessed across experimental treatments of temperature (12 °C, 20 °C) and soil moisture (field-moist, saturated) destructively sampled after three-weeks (T_1) or following three-week recovery period (T_2).

biomass (Figure 3.4B) was strongly related to the original sampling location ($F_{1,33}$ = 17.288, p < 0.001). Total biomass was significantly reduced saturated conditions ($F_{1,33}$ = 8.631, p = 0.006). This was driven by a significant decrease in both soil microfauna ($F_{1,34}$ = 21.152, p < 0.001) and mesofauna ($F_{1,33}$ = 8.266, p = 0.007). Total biomass was not influenced by temperature conditions ($F_{1,33}$ = 0.076, p = 0.784) nor the timing of destructive sampling ($F_{1,33}$ = 1.375, p = 0.249). Soil microfauna biomass was not influenced by significant interaction effects (Appendix E), but total fauna ($F_{1,33}$ = 3.386, p = 0.075) and soil mesofauna ($F_{1,33}$ = 3.439, p = 0.073) biomasses exhibited weak soil moisture by destructive sampling time interaction effects. This suggests that the biomasses of total fauna and soil mesofauna in mesocosms assigned to saturated conditions tended to increase from T_1 to T_2 following a three-week return to initial field-moist conditions. Overall, mean total biomass (± SE) was greatest (0.49 ± 0.10 g of C per m^2 per year) in mesocosms assigned to 12 °C field-moist conditions, sampled at T_1 and was least (0.25 ± 0.07 g of C per m^2 per year) in those assigned to 12 °C saturated conditions, sampled at T_1 (see Appendix D). Estimates of effect size based on a linear model are given in Appendix F.

3.6 Community Composition and Similarity Among Treatments

Reductions in total fauna abundance under saturated soil moisture conditions were driven by Mesostigmata, Collembola, and juvenile and adult oribatid mites at T_1 (Appendix C). In all cases the reductions under saturated conditions were more pronounced at 12 °C than 20 °C, with Collembola completely absent in 12 °C saturated mesocosms. Warmer temperatures slightly increased juvenile Oribatida. Thus, moisture conditions had a significant effect (PerMANOVA $F_{1,17}$ = 3.23, p= 0.045) on the overall community composition of the fauna (Figure 3.5A). Mesocosms were also significant different depending on where they were initially sampled (i.e., block effect PerMANOVA $F_{1,17}$ = 4.35, p= 0.009). Temperature did not significantly affect community composition; however, the community was much more homogeneous under warmed (20 °C) conditions (Figure 3.5B).

The soil food web fauna remained significantly different between the mesocosms that received saturated conditions vs. those under field-moist conditions even after three weeks recovery (T_2) time (Moisture effect PerMANOVA $F_{1,18}$ = 5.64, p= 0.003; Figure 3.6A). The experimental effects of temperature treatment did not significantly affect the soil fauna community

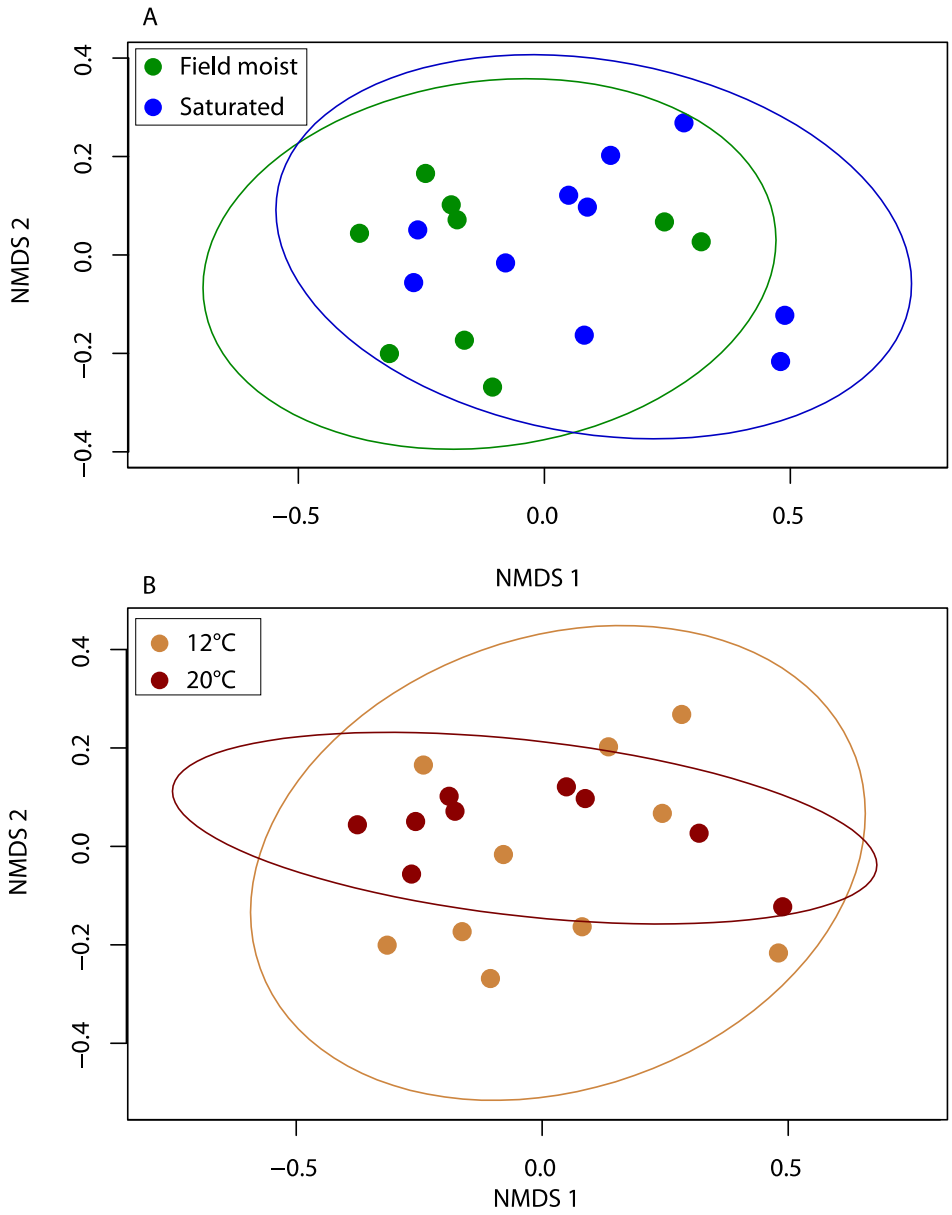

Figure 3.5 Non-metric multidimensional scaling plot of mesocosm similarity at T_1.

(A) mesocosms show significant dissimilarity in community composition between field-moist and saturated moisture conditions; (B) mesocosms show similarity in community composition between temperature treatments. Stress = 0.114. Ellipses represent 95% CI based on similarity between samples.

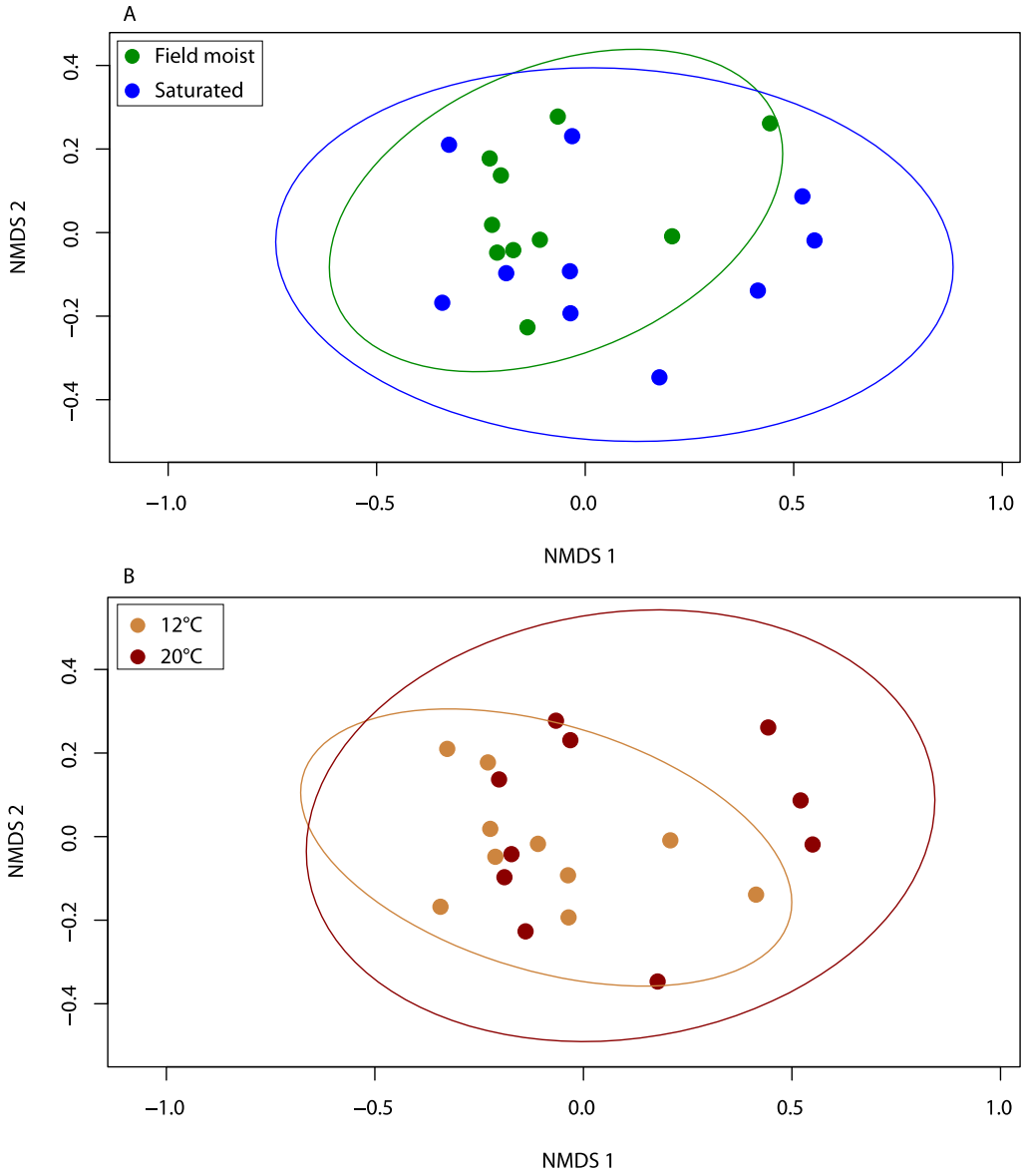

Figure 3.6 Non-metric multidimensional scaling plot of mesocosm similarity at T_2.

(A) mesocosms show significant dissimilarity in community composition between field-moist and saturated moisture conditions; (B) mesocosms show similarity in community composition between temperature treatments. Stress=0.146. Ellipses represent 95% CI based on similarity between samples.

composition, and the trend towards homogeneity under increased temperature treatment was not observed following the T_2 recovery period (Figure 3.6B).

3.7 Soil Food Web Carbon and Nitrogen Flux

Mean total consumptive flux, C mineralization, and N mineralization were compared across 39 mesocosms. Mean total consumptive flux ($W = 0.988$, $p = 0.944$), C mineralization ($W = 0.987$, $p = 0.933$), and N mineralization ($W = 0.981$, $p = 0.751$) met the assumption of normality, per a Shapiro-Wilk test. Mean total consumptive flux ($F_{7,31} = 0.719$, $p = 0.657$), C mineralization ($F_{7,31} = 0.747$, $p = 0.635$), and N mineralization ($F_{7,31} = 0.847$, $p = 0.558$) also met the assumption of homogeneity of variance, per Levene's test.

Mean total consumptive flux of C through the soil fauna food web (Figure 3.7A) was significantly related to block effects ($F_{1,33} = 6.267$, $p = 0.017$), and was greater in blocks characterized by especially high soil fauna abundances. Total C flux also significantly decreased under saturation ($F_{1,33} = 8.653$, $p = 0.006$), but significantly increased at 20 °C vs. 12 °C ($F_{1,33} = 214.881$, $p < 0.001$). This was driven by a significant temperature-by-sampling time interaction effect ($F_{1,33} = 94.744$, $p < 0.001$), which highlights that mean total flux in mesocosms assigned to 20 °C decreased at T_2 following a three-week return to 12 °C field-moist conditions. Destructive sampling treatments alone did not significantly affect C flux ($F_{1,33} = 0.748$, $p = 0.393$). No other interaction effects significantly affected C flux (Appendix E). Mean total flux (± SE) under each treatment is presented in Appendix D. Estimates of effect size based on a linear model are given in Appendix F.

Total C mineralization of the soil food web (Figure 3.7B) followed similar trends to total C flux whereby experimental block effects were significant ($F_{1,33} = 6.173$, $p = 0.018$). Total C mineralization increased at 20 °C vs. 12 °C ($F_{1,33} = 236.901$, $p < 0.001$), but decreased under saturated vs. field-moist soil moisture conditions ($F_{1,33} = 8.725$, $p = 0.006$). Destructive sampling treatments alone did not affect C mineralization ($F_{1,33} = 0.739$, $p = 0.396$), but C mineralization was influenced by a significant temperature by destructive sampling time interaction effect ($F_{1,33} = 105.313$, $p < 0.001$), highlighting that total C mineralization in mesocosms assigned to 20 °C decreased at T_2 following a three-week return to 12 °C field-moist conditions. No other

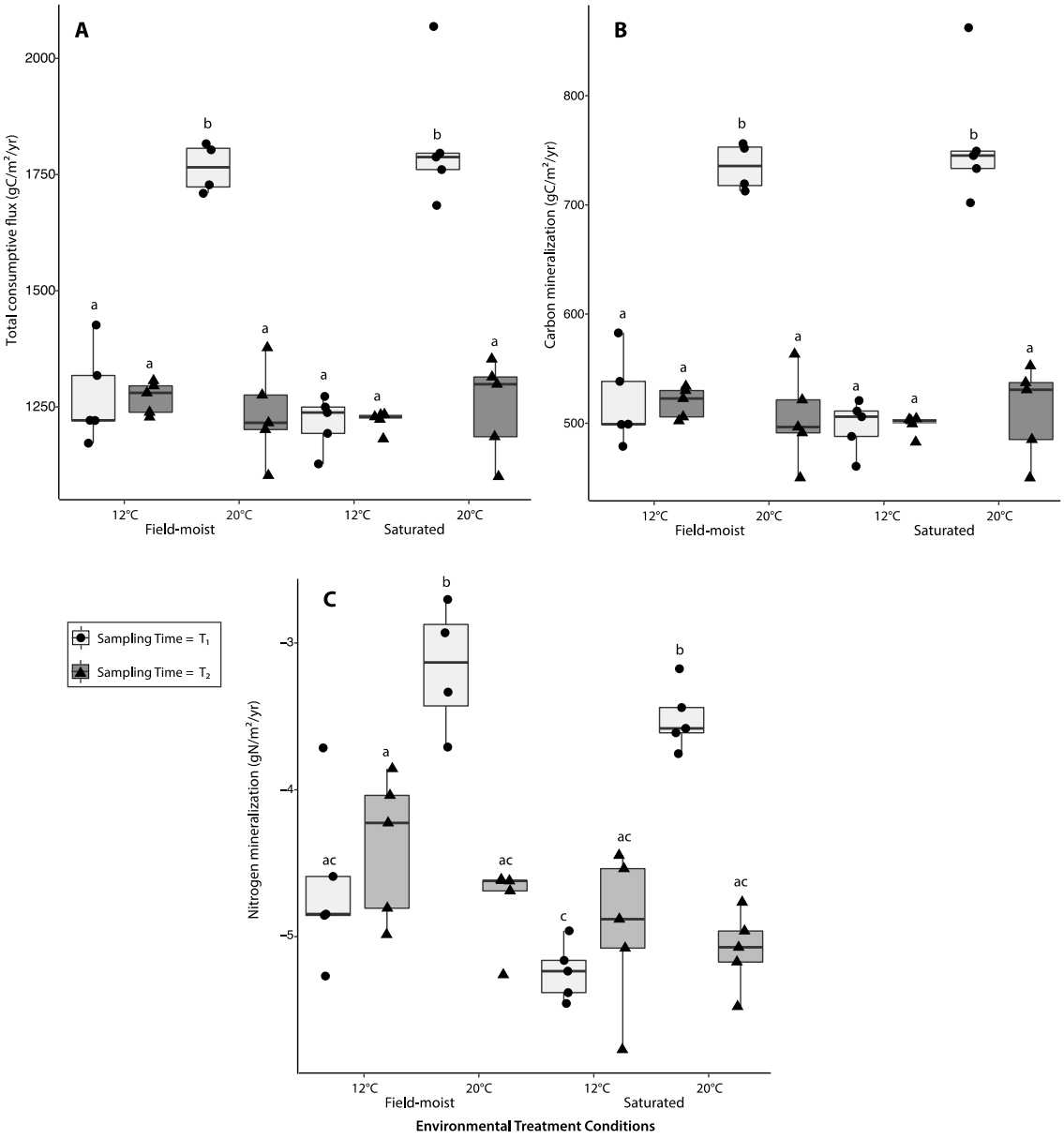

Figure 3.7 Modeled rates of (A) carbon flux (consumption), (B) carbon mineralization (respiration), and (C) nitrogen mineralization.

Fluxes were modeled across experimental treatments of temperature (12 °C, 20 °C) and soil moisture (field-moist, saturated) destructively sampled after three-weeks (T_1) or following three-week recovery period (T_2). Letters denote significant differences between groups, as per Tukey's HSD test.

interaction effects significantly influenced C mineralization (Appendix E). Following three weeks of assigned experimental soil moisture and temperature conditions at T_1 destructive sampling, C mineralization represented ~41% of total flux in mesocosms assigned to 12 °C conditions, and 42% of total flux in mesocosms assigned to 20 °C conditions. For all mesocosms, during the three weeks of recovery under field (12 °C field-moist) conditions (i.e., T_2 destructive sampling), C mineralization remained at ~41% of the total flux. Mean total C mineralization (± SE) under each treatment is presented in Appendix D. Estimates of effect size based on a linear model are given in Appendix F.

Mean total N mineralization (Figure 3.7C) was significantly influenced by both soil moisture ($F_{1,33} = 13.061$, $p = 0.001$) and temperature ($F_{1,33} = 78.383$, $p < 0.001$) conditions; mean total N mineralization decreased under saturated field-moist vs. conditions and increased at 20 °C vs.12 °C. Furthermore, a significant temperature by destructive sampling time interaction effect ($F_{1,33} = 54.875$, $p < 0.001$) demonstrates that mean total N mineralization in mesocosms assigned to 20 °C decreased at T_2 following a three-week return to 12 °C field-moist conditions. There were no significant block effects ($F_{1,33} = 0.002$, $p = 0.965$) and destructive sampling treatments did not affect N mineralization ($F_{1,33} = 2.387$, $p = 0.132$). No other interaction effects significantly affected N mineralization (Appendix E). Mean total N mineralization (± SE) under each treatment is presented in Appendix D. Estimates of effect size based on a linear model are given in Appendix F.

Chapter 4

4 Discussion

Soil food web stability is thought to be underpinned by high diversity and relatively complex trophic interactions among trophic groups (de Castro et al., 2021). Using a mesocosm experiment I observed direct changes to the soil food web driven by a sudden shift in soil moisture saturation, and to a less extent high soil temperature, that altered how C and N were transferred and transformed through the soil food web. Soil saturation had a greater effect on soil mesofauna than soil microfauna, while temperature had a greater effect on the C and N fluxes than the actual biomass of organisms. When experimental mesocosms were allowed to slowly returned to control temperature conditions, so did the soil food web and the corresponding C and N flux; however, mesocosms assigned to field-moist soil conditions did not fully recover during the allotted three-weeks recovery period, and saturated soil conditions continued to influence the soil fauna.

4.1 System Resistance

Whether a system resists change under a perturbation and whether, or how long, a system takes to return to previous conditions following change are two aspects of systems stability (Allison and Martiny, 2008). Microbial phenol oxidase and peroxidase activities were resistant to saturation, but significantly increased under +8 °C warming. This finding is consistent with the expected relationship between temperature and biological activity defined by enzyme kinetics, which suggests that enzyme activity increases with temperature as a function of increased biological activity to a point of a physio-thermal optimum where enzymes and substrate then begin to degrade (Peterson et al., 2007). Furthermore, this is partially consistent with the findings of Thakur et al. (2021), who suggest that short-term perturbations have an effect on soil fauna and the microbial communities they consume, and Allison and Martiny (2008), who suggest that soil microbial communities are generally affected by short-term environmental change.

Mean total soil fauna abundances monotonically decreased over the duration of the experiment, indicating that experimental effects may limit the power with which statistical tests can detect experimentally induced changes in total abundance. However, mean total soil fauna abundance

was significantly reduced under saturated vs. field-moist conditions. Decreases in total soil fauna abundance under saturation were driven by corresponding decreases in both soil microfauna and mesofauna abundances. There are differences in ecology between these groups of soil fauna, as microfauna in soils tend to be aquatic and occupy water-filled pores and water films surrounding soil particles (Weston and Whittaker, 2004), whereas soil mesofauna inhabit soil pore spaces; however, anoxic conditions had a strong effect on both groups. Saturation also drove corresponding changes in soil fauna community composition at T_1 sampling, which further highlights the low resistance of soil fauna under saturated conditions. Thus, hydrological conditions (i.e. drought vs. saturation) may be an important driver of changes in soil fauna abundances in fungal-dominated systems (Zhang et al., 2022). Total soil fauna abundance, total soil microfauna abundance, and total soil mesofauna abundance were each resistant under warming. However, juvenile oribatid abundances increased slightly under warming. This is consistent with the increases in small-bodied soil fauna abundances reported by Lindo (2015); the weaker response observed in the present study may be an effect of differences in the length of the experiment. Mesofauna were also influenced by a significant temperature by destructive sampling interaction, which may suggest that soil mesofauna communities recovered following these changes in juvenile oribatid abundances. Overall, biological activity (e.g., metabolic processes) is inhibited under low temperatures (Carrera et al., 2009), and increases with increasing temperature (Brown et al., 2004). Thus, increased abundances under increased temperature is likely a metabolic response in growth and reproduction among the soil fauna. Lack of habitable pore space under saturated soil moisture conditions likely limited this response. It is likely that enhanced soil moisture conditions that do not severely restrict available habitable soil pore spaces (Tsiafouli et al., 2005; Turnbull and Lindo, 2015) may further enhance the effects of temperature on soil fauna abundances vs. conditions where soil systems become drier and soil moisture is limiting.

4.2 System Resilience

Mesocosm microbial activity showed a high degree of resilience. The microbial community recovered following warming-associated increases in activity, as highlighted by significant temperature by destructive sampling treatment interaction effects on both phenol oxidase and peroxidase activity. However, Thakur et al. (2021), suggest that a short-term perturbation is more

detrimental to the resilience of microbes than microbial consumers. Throughout the experiment, microbial activity was highly variable, especially at T_1. This variability in microbial activity limits the direct comparison of the resilience of the microbial community to its consumers in the present experiment.

Soil fauna exhibited low resilience, as neither total fauna, soil microfauna, nor soil mesofauna communities recovered following saturation-associated decreases in abundance. This is evident from the lack of significant corresponding soil moisture by destructive sampling time interactions. Changes in soil fauna community composition at T_1 were maintained at T_2, which further highlights the low resilience of the soil fauna. This is consistent with previous findings that suggest fungal-dominated soil systems, like the peatland system examined here, do not demonstrate especially strong resilience (de Vries et al., 2012). The mean total faunal abundance under each combination of soil moisture and temperature conditions at T_2 was significantly less than at T_0. However, this may be more indicative of the laboratory-based mesocosm context of the experiment than under field conditions, as soil fauna abundances decreased monotonically over the duration of the experiment across all treatment groups. Alternatively, this may also suggest that communities did recover across all treatment groups. In the larger mesocosm experiment, mean total abundance was less variable at T_2 than T_1. This may suggest that mesocosms tended to recover from experimentally manipulated conditions but returned to a new stable state, demonstrated by more similar mean total abundances between treatment groups following the three-week period of 12 °C field-moist conditions and less variation in total abundances between and across treatments.

Corresponding to trends in total soil fauna abundances, total microfauna and mesofauna abundances significantly decreased between sampling at T_2 and T_0. This is partially consistent with the findings of de Vries et al. (2012), and may suggest that mesocosms are not stable for culturing a whole soil food web.

4.3 Carbon and Nutrient Fluxes

Total consumptive flux significantly decreased under saturated vs. field moist conditions, corresponding to a weak reduction in soil fauna total biomass under saturated conditions. This

finding is consistent with previous research that suggests that high levels moisture in soils drive reductions in the habitable pore space of soil that can reduce soil fauna biomass (Tsiafouli et al., 2005; Turnbull and Lindo, 2015). However, the lack of a significant soil moisture-by-sampling time interaction suggests that consumption in mesocosms assigned to saturated conditions did not increase following a three-week return to 12 °C field-moist conditions. This suggests that the mesocosms were overall not resilient to hydrology-mediated changes in C fluxes.

Although total biomass was not affected by imposed temperature conditions, total modelled C flux corresponding to consumption increased at 20 °C vs. 12 °C. This increase in flux was driven by the increased modelled metabolic demand of each node, consistent with the metabolic theory of ecology (Brown et al., 2004). In the energetic model of the system, the increased metabolic demand of each node was manipulated through changes in three model parameters: assimilation efficiency, production efficiency, and turnover (Appendix A). A significant temperature-by-sampling time interaction highlights that total C flux declined following a three-week return to 12 °C field-moist conditions when the metabolic demand was reduced. This suggests that ecosystem function recovered following warming mediated increases in total C flux.

Following trends in total consumption, total modelled C mineralization also significantly decreased under saturated vs. field-moist conditions, but significantly increased at 20 °C vs. 12 °C. Because overall C storage is the difference of total consumption less C mineralization, this suggests that total C storage may increase under warming, corresponding to increased consumption, but at a decreasing rate per unit biomass, corresponding to increased soil heterotrophic respiration under increased metabolic demand. Similarly, mesocosm respirometry results showed mean heterotrophic respiration was influenced by temperature, but not soil moisture; yet empirical C mineralization rates were not similar between the measured and modelled data. In the energetic model of the system, the system is assumed to be in an energetic equilibrium such that consumption is calculated to exactly meet the costs of metabolic demands (Moore and de Ruiter, 2012; Buchkowski et al., 2023). Following the simulated perturbation represented by assigned soil moisture and temperature conditions, the system may have fallen out of energetic equilibrium such that consumption was no longer in balance with energetic

demands, resulting in these differences in trends between modelled C mineralization and observed soil heterotrophic respiration.

Total N mineralization was negative across all combinations of experimental treatments, indicative of overall net N-immobilization as organic N within the soil food web. Total N mineralization similarly decreased under saturated vs. field-moist conditions, but increased at 20 °C vs. 12 °C. The lack of a significant soil moisture-by-sampling time interaction suggests that N mineralization in mesocosms assigned to saturated conditions did not increase following a three-week return to 12 °C field-moist conditions. This suggests that the mesocosms were overall not resilient following hydrology-mediated changes in N fluxes. However, mesocosm total N mineralization was affected by a significant temperature-by-sampling time interaction, highlighting that N mineralization in mesocosms assigned to 20 °C decreased following a three-week return to 12 °C field-moist conditions. This suggests that the mesocosms were overall somewhat resilient following temperature-mediated changes in N fluxes. Finally, Staddon et al. (2010) suggests that top microarthropod predators drive N mineralization, and arthropod-feeding Mesostigmata slightly declined at T_1 under saturated conditions, but so did their prey. This suggests that increased growth rates under warming for prey species may increase N immobilization within faunal biomass, but losses in fauna biomass under saturation do not general affect N mineralization rates.

4.4 Caveats, Challenges and Limitations

The mesocosm design component of the experimental design of this study was constrained by both spatial and temporal limitations. For example, because fungal resistance is thought to be driven by higher fungal biomass (Cole et al., 2006), the low observed resistance in the fungal energy channel may again be an effect of the physical spatial scale of individual mesocosms. Similarly, because the lack of a significant effect of destructive sampling time on soil moisture suggests that mesocosms assigned to saturated conditions did not fully return to field-moist conditions over the three-week recovery period. Thus, the observed low resistance in the soil fauna communities of the present study may be the result of a slower than expected response to experimental conditions.

The analysis of the microbial community in the present study was also limited because I did not track microbial communities per se, but rather inferred microbial activity from enzyme activity and heterotrophic respiration. Modelled estimates of consumption, C mineralization, and N mineralization are similarly limited as the microbial biomasses used to parameterize these models are derived from previous research at the site (Lyons and Lindo, 2020) and do not reflect any microbial biomass changes that may have occurred during the experiment. Bacterial and fungal biomass have previously been shown to respond differently to warming with increases in bacterial biomass, and fungal biomass being impacted and declining under warming (Asemaninejad et al., 2019). However, few studies have explored how different microbial communities respond to short-term changes in soil moisture, including saturation. Field observation studies suggest both fungal and bacterial communities shift with vertical distribution in relation to water table (Asemaninejad et al., 2017, 2019). Given that an estimated ~90% of fluxes in the soil food web were derived from the microbial community, it is important for future models to accurately track the microbial community. For example, phospholipid fatty acid (PLFA) analysis could be used in similar mesocosm studies to estimate changes in the biomass of microbial soil food web nodes, including bacteria, fungi, and protists.

The energetic food web model approach (*sensu* Moore and de Ruiter, 2012) has several assumptions and caveats. First, as suggested above, the model assumes the system is at equilibrium when calculating fluxes, which may not be the case in an environmental change experiment. The output of the model is also dependent on the parameter inputs of assimilation efficiency (E_a), production efficiency (E_p) and non-consumptive death or population turnover rate (d). These parameters are mostly from the literature provided by work original publications on soil food web modelling (e.g., Hunt et al., 1987), and have largely not been critically examined, or measured for specific systems such as peatlands. Both production efficiency (E_p) and non-consumptive death (d) were scaled for increased metabolic demands under warming, which is fairly predictable under the metabolic theory of ecology (Brown et al., 2004), and these metabolic costs were largely responsible for differences in model C and N outputs in the model. Thus, further research examining taxon-specific trophic efficiencies alongside better estimates of population turnover would greatly benefit model parameterization.

4.5 Conclusions and Significance

The soil food web performs the important ecological function of decomposition, leading to C and N transformations, including C and N mineralization. Despite relatively low amounts of C mineralization compared to other systems such as forest and grasslands (c), these systems store a large amount of C because productivity exceeds rates of heterotrophic respiration. Both abiotic (e.g. moisture, temperature) and biotic (e.g. metabolic efficiency) factors help limit rates of heterotrophic respiration in boreal peatlands. Boreal peatlands are typically considered cool and wet environments, yet under climate change, we expect that short-term perturbations, characterized by extreme soil moisture and temperature conditions, will become more common (IPCC, 2018). These perturbations threaten the stability and C storage of boreal peatland soil systems. I demonstrate that reduced resistance of the soil food web was largely driven by changes in imposed soil moisture treatments. Hydrology has been overlooked as a factor in other studies examining soil food web resistance and resilience following a perturbation (Thakur et al., 2021) and should be considered more in future studies. My findings also suggest that a short-term perturbation drives changes in fungal activity (i.e., phenol oxidase concentration), but moreover, that the arthropod component of the soil food web is not resistant to soil saturation. Finally, I demonstrate that C storage may increase under warming, corresponding to increases in soil food web consumption, but at a decreasing rate per unit biomass, corresponding to increases in C mineralization. This is consistent with previous research that suggests climate change threatens to drive soils to change from a C sink to a C source (Bragazza et al., 2013; Crowther et al., 2016; Harenda et al., 2018).

The increasing likelihood of extreme climate events predicted for the next century is expected to have major impacts on biodiversity at local scales (Garcia et al., 2014), and changes in both global temperatures and precipitation regimes may drive changes to the microclimate of future soils (Tarnocai et al., 2009), with cascading effects on soil fauna, the overall structure of soil food webs, and ultimately C and N cycling. Quantifying and modeling how changes in belowground biodiversity under climate warming affect soil C and N is an important first step in predicting C storage potential in boreal peatlands under future climate scenarios. While there is evidence that soil fauna are important drivers of carbon and nutrient transformations, few studies specifically focus on the energetics of soil fauna communities under global climate change.

Carbon is the energetic currency that is transferred from one trophic group to another via consumption, however, the process of trophic transfer is inefficient (Hunt et al., 1987), as C is lost from the food web due to metabolic and other biological processes. Global change factors can therefore affect C and N flux both directly and indirectly through changes in metabolism, especially under warming, and changes in trophic group biomass. Changes in trophic group biomass that result in losses of biodiversity may also rewire food web topology, and future research should consider both how changes in the topology of a food web may affect overall flux, as well as whether energetic approaches based on metabolic theory are valid under warming. This is especially true in highly organic system such as peatlands that are reservoirs for C storage and soil biodiversity, while also having high potential for climate change impacts.

Metabolic rate controls ecological processes both at the level of the population (e.g., metabolic rate vs. biomass production) and at the level of the ecosystem (e.g., metabolic rate vs. trophic dynamics). As such, whether soil C is retained within the soil system or is released back to the atmosphere depends largely on the topology of the soil food web and the efficiency at which the organic inputs are decomposed by the soil food web, as well as the temperature of the system. Here I demonstrate that interacting global change factors that have opposing effects on soil biodiversity may lead to antagonistic interactions between global change factors at the ecosystem-level (i.e. C and N transformations). Both temperature and soil moisture conditions are anticipated to change under global climate change and are the primary drivers of soil invertebrate population dynamics (Goncharov et al., 2023) and thus understanding the interactions among these multiple drivers of soil communities is the first step (Rillig et al., 2019), however, understanding the relationship between changes in soil communities and ecosystem-level processes requires an energetic perspective.

References

Allison, S.D., Martiny, J.B.H., 2008. Resistance, resilience, and redundancy in microbial communities. Proceedings of the National Academy of Sciences 105, 11512–11519. doi:10.1073/pnas.0801925105

Andrássy, I., 1956. Die rauminhalst and gewichtsbestimmung der fadenwurmer (Nematoden). Acta ZoologicaAcademi Sciences, Hungary 2, 1–15.

Asemaninejad, A., Thorn, R.G., Branfireun, B.A., Lindo, Z., 2019. Vertical stratification of peatland microbial communities follows a gradient of functional types across hummock-hollow microtopographies. Ecoscience 26, 249–258. doi:10.1080/11956860.2019.1595932

Asemaninejad, A., Thorn, R.G., Lindo, Z., 2017. Vertical distribution of fungi in hollows and hummocks of boreal peatlands. Fungal Ecology 27, 59–68. doi:10.1016/J.FUNECO.2017.02.002

Barreto, C., Branfireun, B.A., McLaughlin, J.W., Lindo, Z., 2021. Responses of oribatid mites to warming in boreal peatlands depend on fen type. Pedobiologia 89, 150772. doi:https://doi.org/10.1016/j.pedobi.2021.150772

Barreto, C., Lindo, Z., 2021. Checklist of oribatid mites (Acari: Oribatida) from two contrasting boreal fens: An update on oribatid mites of Canadian peatlands. Systematic and Applied Acarology 26, 866–884. doi:10.11158/saa.26.5.4

Barreto, C., Lindo, Z., 2018. Drivers of decomposition and the detrital invertebrate community differ across a hummock-hollow microtopology in Boreal peatlands. Écoscience 25, 39–48. doi:10.1080/11956860.2017.1412282

Batjes, N.H., 1996. Total carbon and nitrogen in the soils of the world. European Journal of Soil Science 47, 151–163. doi:https://doi.org/10.1111/j.1365-2389.1996.tb01386.x

Beaulne, J., Garneau, M., Magnan, G., Boucher, É., 2021. Peat deposits store more carbon than trees in forested peatlands of the boreal biome. Scientific Reports 11. doi:10.1038/s41598-021-82004-x

Bian, H., Li, C., Zhu, J., Xu, L., Li, M., Zheng, S., He, N., 2022. Soil moisture affects the rapid response of microbes to labile organic C addition. Frontiers in Ecology and Evolution 10. doi:10.3389/fevo.2022.857185

Bokhorst, S., Bjerke, J.W., Bowles, F.W., Melillo, J., Callaghan, T. V., Phoenix, G.K., 2008. Impacts of extreme winter warming in the sub-Arctic: Growing season responses of dwarf shrub heathland. Global Change Biology 14, 2603–2612. doi:10.1111/j.1365-2486.2008.01689.x

Bragazza, L., Freeman, C., Jones, T., Rydin, H., Limpens, J., Fenner, N., Ellis, T., Gerdol, R., Hájek, M., Hájek, T., Iacumin, P., Kutnar, L., Tahvanainen, T., Toberman, H., 2006. Atmospheric nitrogen deposition promotes carbon loss from peat bogs. Proceedings of the National Academy of Sciences 103, 19386–19389. doi:10.1073/pnas.0606629104

Bragazza, L., Parisod, J., Buttler, A., Bardgett, R.D., 2013. Biogeochemical plant-soil microbe feedback in response to climate warming in peatlands. Nature Climate Change 3, 273–277. doi:10.1038/nclimate1781

Brown, J., Gillooly, J.F., Allen, A.P., Savage, V.M., West, G.B., 2004. Toward a metabolic theory of ecology. Ecology 85, 1771–1789. doi:10.1016/B978-0-12-814612-5.00011-7

Buchkowski, R.W., Barel, J.M., Jassey, V.E.J., Lindo, Z., 2022. Cannibalism has its limits in soil food webs. Soil Biology and Biochemistry 172, 108773. doi:10.1016/J.SOILBIO.2022.108773

Buchkowski, R.W., Barreto, C., Lindo, Z., 2023. soilfoodwebs: An R package for analyzing and simulating nutrient fluxes through food webs. R package version 1.0.2, [WWW Document]. URL https://CRAN.R-project.org/package=soilfoodwebs. (accessed 7.9.23).

Carrera, N., Barreal, M.E., Gallego, P.P., Briones, M.J.I., 2009. Soil invertebrates control peatland C fluxes in response to warming. Functional Ecology 23, 637–648. doi:https://doi.org/10.1111/j.1365-2435.2009.01560.x

Cole, L., Bradford, M.A., Shaw, P.J.A., Bardgett, R.D., 2006. The abundance, richness and functional role of soil meso- and macrofauna in temperate grassland—A case study. Applied Soil Ecology 33, 186–198. doi:10.1016/J.APSOIL.2005.11.003

Crowther, T.W., Todd-Brown, K.E.O., Rowe, C.W., Wieder, W.R., Carey, J.C., MacHmuller, M.B., Snoek, B.L., Fang, S., Zhou, G., Allison, S.D., Blair, J.M., Bridgham, S.D., Burton, A.J., Carrillo, Y., Reich, P.B., Clark, J.S., Classen, A.T., Dijkstra, F.A., Elberling, B., Emmett, B.A., Estiarte, M., Frey, S.D., Guo, J., Harte, J., Jiang, L., Johnson, B.R., Kroël-Dulay, G., Larsen, K.S., Laudon, H., Lavallee, J.M., Luo, Y., Lupascu, M., Ma, L.N., Marhan, S., Michelsen, A., Mohan, J., Niu, S., Pendall, E., Peñuelas, J., Pfeifer-Meister, L., Poll, C., Reinsch, S., Reynolds, L.L., Schmidt, I.K., Sistla, S., Sokol, N.W., Templer, P.H., Treseder, K.K., Welker, J.M., Bradford, M.A., 2016. Quantifying global soil carbon losses in response to warming. Nature 540, 104–108. doi:10.1038/nature20150

de Castro, F., Adl, S.M., Allesina, S., Bardgett, R.D., Bolger, T., Dalzell, J.J., Emmerson, M., Fleming, T., Garlaschelli, D., Grilli, J., Hannula, S.E., de Vries, F., Lindo, Z., Maule, A.G., Öpik, M., Rillig, M.C., Veresoglou, S.D., Wall, D.H., Caruso, T., 2021. Local stability properties of complex, species-rich soil food webs with functional block structure. Ecology and Evolution 11, 16070–16081. doi:https://doi.org/10.1002/ece3.8278

de Vries, F.T., Caruso, T., 2016. Eating from the same plate? Revisiting the role of labile carbon inputs in the soil food web. Soil Biology and Biochemistry 102, 4–9. doi:10.1016/J.SOILBIO.2016.06.023

de Vries, F.T., Liiri, M.E., Bjørnlund, L., Bowker, M.A., Christensen, S., Setälä, H.M., Bardgett, R.D., 2012. Land use alters the resistance and resilience of soil food webs to drought. Nature Climate Change 2, 276–280. doi:10.1038/nclimate1368

Dieleman, C.M., Branfireun, B.A., Mclaughlin, J.W., Lindo, Z., 2015. Climate change drives a shift in peatland ecosystem plant community: Implications for ecosystem function and stability. Global Change Biology 21, 388–395. doi:10.1111/gcb.12643

Digel, C., Curtsdotter, A., Riede, J., Klarner, B., Brose, U., 2014. Unravelling the complex structure of forest soil food webs: higher omnivory and more trophic levels. Oikos 123, 1157–1172. doi:https://doi.org/10.1111/oik.00865

Edwards, C.A., 1967. Relationship between weights, volumes and numbers of soil animals, in: Graff, O., Satchell, J.J. (Eds.), Progress in Soil Biology, Proceedings of a Colloquium on the Dynamics of Soil Communities. Friedr. Vieweg. Amsterdam, Braunscheweig-Voelkenrode, Holland, pp. 585–594.

Forge, T.A., Kimpinski, J., 2008. Nematodes, in: Carter, M.R., Gregorich, E.G. (Eds.), Soil Sampling and Methods of Analysis. CRC Press Taylor & Francis, Boca Raton, FL, USA, pp. 415–426.

Garcia, R.A., Cabeza, M., Rahbek, C., Araújo, M.B., 2014. Multiple dimensions of climate change and their implications for biodiversity. Science 344, 1247579. doi:10.1126/science.1247579

Gessler, A., Schaub, M., McDowell, N.G., 2017. The role of nutrients in drought-induced tree mortality and recovery. New Phytologist. doi:10.1111/nph.14340

Gilman, S.E., Urban, M.C., Tewksbury, J., Gilchrist, G.W., Holt, R.D., 2010. A framework for community interactions under climate change. Trends in Ecology and Evolution 25, 325–331. doi:10.1016/j.tree.2010.03.002

Gladstone-Gallagher, R. V., Pilditch, C.A., Stephenson, F., Thrush, S.F., 2019. Linking traits across ecological scales determines functional resilience. Trends in Ecology and Evolution. doi:10.1016/j.tree.2019.07.010

Goncharov, A.A., Leonov, V.D., Rozanova, O.L., Semenina, E.E., Tsurikov, S.M., Uvarov, A. V., Zuev, A.G., Tiunov, A. V., 2023. A meta-analysis suggests climate change shifts structure of regional communities of soil invertebrates. Soil Biology and Biochemistry 181, 109014. doi:10.1016/J.SOILBIO.2023.109014

González-Macé, O., Scheu, S., 2018. Response of collembola and acari communities to summer flooding in a grassland plant diversity experiment. PLoS ONE 13. doi:10.1371/journal.pone.0202862

Gore, A.J.P., 1984. Mires: Swamp, Bog, Fen and Moor. Ecosystems of the World 4, 440–478. doi:https://doi.org/10.1002/iroh.19840690318

Gorham, E., 1991. Northern peatlands: role in the carbon cycle and probable responses to climatic warming. Ecological Applications 1, 182–195. doi:https://doi.org/10.2307/1941811

Griffiths, B.S., Philippot, L., 2013. Insights into the resistance and resilience of the soil microbial community. FEMS Microbiology Reviews. doi:10.1111/j.1574-6976.2012.00343.x

Harenda, K.M., Lamentowicz, M., Samson, M., Chojnicki, B.H., 2018. The role of peatlands and their carbon storage function in the context of climate change, in: Zielinski, T., Sagan, I., Surosz, W. (Eds.), Interdisciplinary Approaches for Sustainable Development Goals: Economic Growth, Social Inclusion and Environmental Protection. Springer International Publishing, Cham, pp. 169–187. doi:10.1007/978-3-319-71788-3_12

Haustein, K., Allen, M.R., Forster, P.M., Otto, F.E.L., Mitchell, D.M., Matthews, H.D., Frame, D.J., 2017. A real-time Global Warming Index. Scientific Reports 7, 15417. doi:10.1038/s41598-017-14828-5

Hillebrand, H., Kunze, C., 2020. Meta-analysis on pulse disturbances reveals differences in functional and compositional recovery across ecosystems. Ecology Letters 23, 575–585. doi:10.1111/ele.13457

Holmstrup, M., Damgaard, C., Schmidt, I.K., Arndal, M.F., Beier, C., Mikkelsen, T.N., Ambus, P., Larsen, K.S., Pilegaard, K., Michelsen, A., Andresen, L.C., Haugwitz, M., Bergmark, L., Priemé, A., Zaitsev, A.S., Georgieva, S., Dam, M., Vestergård, M., Christensen, S., 2017. Long-term and realistic global change manipulations had low impact on diversity of soil biota in temperate heathland. Scientific Reports 7. doi:10.1038/srep41388

Hunt, H.W., Coleman, D.C., Ingham, E.R., Ingham, R.E., Elliott, E.T., Moore, J.C., Rose, S.L., Reid, C.P.P., Morley, C.R., 1987. The detrital food web in a shortgrass prairie. Biology and Fertility of Soils 3, 57–68. doi:10.1007/BF00260580

Hunt, H.W., Elliott, E.T., Walter, D.E., 1989. Inferring trophic transfers from pulse-dynamics in detrital food webs. Plant and Soil 115, 247–259.

IPCC, 2018. Global warming of 1.5°C. An IPCC Special Report on the impacts of global warming of 1.5°C above pre-industrial levels and related global greenhouse gas emission pathways, in the context of strengthening the global response to the threat of climate change, sustainable development, and efforts to eradicate poverty.

IPCC, 2000. Special Report on Emissions Scenarios. Cambridge University Press, Cambridge, UK.

Isbell, F., Craven, D., Connolly, J., Loreau, M., Schmid, B., Beierkuhnlein, C., Bezemer, T.M., Bonin, C., Bruelheide, H., De Luca, E., Ebeling, A., Griffin, J.N., Guo, Q., Hautier, Y., Hector, A., Jentsch, A., Kreyling, J., Lanta, V., Manning, P., Meyer, S.T., Mori, A.S., Naeem, S., Niklaus, P.A., Polley, H.W., Reich, P.B., Roscher, C., Seabloom, E.W., Smith, M.D., Thakur, M.P., Tilman, D., Tracy, B.F., Van Der Putten, W.H., Van Ruijven, J., Weigelt, A., Weisser, W.W., Wilsey, B., Eisenhauer, N., 2015. Biodiversity increases the resistance of ecosystem productivity to climate extremes. Nature 526, 574–577. doi:10.1038/nature15374

IUCN, 2021. IUCN 2021 annual report. Gland, Switzerland.

Kamath, D., Barreto, C., Lindo, Z., 2022. Nematode contributions to the soil food web trophic structure of two contrasting boreal peatlands in Canada. Pedobiologia 93–94. doi:10.1016/j.pedobi.2022.150809

Kuriki, G., 2008. The life cycle of *Limnozetes ciliatus* (Schrank, 1803) (Acari: Oribatida). Journal of the Acarological Society of Japan 17, 75–85. doi:10.2300/acari.17.75

Lebrun, P., 1971. Écologie et biocénotique de quelques peuplements d'arthropodes édaphiques, Mémoires du Musée royal d'histoire naturelle de Belgique = Verhandelingen van het Koninklijk Natuurhistorisch Museum van Belgie. Institut Royal des Sciences Naturelles de Belgique.

LeCraw, R.M., Kratina, P., Srivastava, D.S., 2014. Food web complexity and stability across habitat connectivity gradients. Oecologia 176, 903–915.

Li, J., Wang, G., Mayes, M.A., Allison, S.D., Frey, S.D., Shi, Z., Hu, X.M., Luo, Y., Melillo, J.M., 2019. Reduced carbon use efficiency and increased microbial turnover with soil warming. Global Change Biology 25, 900–910. doi:10.1111/gcb.14517

Li, Y., Shi, C., Wei, D., Ding, J., Xu, N., Jin, L., Wang, L., 2023. Associations of soil bacterial diversity and function with plant diversity in Carex tussock wetland. Frontiers in Microbiology 14. doi:10.3389/fmicb.2023.1142052

Liiri, M., Setälä, H., Haimi, J., Pennanen, T., Fritze, H., 2002. Relationship between soil microarthropod species diversity and plant growth does not change when the system is disturbed. Oikos 96, 137–149. doi:https://doi.org/10.1034/j.1600-0706.2002.960115.x

Limpens, J., Berendse, F., Blodau, C., Canadell, J.G., Freeman, C., Holden, J., Roulet, N., Rydin, H., Schaepman-Strub, G., 2008. Peatlands and the carbon cycle: from local processes to global implications – a synthesis. Biogeosciences 5, 1475–1491. doi:10.5194/bg-5-1475-2008

Lindo, Z., 2015. Warming favours small-bodied organisms through enhanced reproduction and compositional shifts in belowground systems. Soil Biology and Biochemistry 91, 271–278. doi:10.1016/j.soilbio.2015.09.003

Luo, Y., Zhou, X., 2006. CHAPTER 6 - Temporal and spatial variations in soil respiration, in: Luo, Y., Zhou, X. (Eds.), Soil Respiration and the Environment. Academic Press, Burlington, pp. 107–131. doi:https://doi.org/10.1016/B978-012088782-8/50006-1

Luxton, M., 1981. Studies on the oribatid mites of a Danish beech wood soil. VII. Energy budgets. Pedobiologia.

Luxton, M., 1972. Studies of the oribatid mites of a Danish beech wood soil. I. Nutritional biology. Pedobiologia.

Lyons, C.L., Lindo, Z., 2020. Above- and belowground community linkages in boreal peatlands. Plant Ecology 221, 615–632. doi:10.1007/s11258-020-01037-w

Matthews, H.D., Wynes, S., 2022. Current global efforts are insufficient to limit warming to 1.5°C. Science 376, 1404–1409. doi:10.1126/science.abo3378

McCann, K.S., 2000. The diversity–stability debate. Nature 405, 228–233. doi:10.1038/35012234

McCann, K.S., Rooney, N., 2009. The more food webs change, the more they stay the same. Philosophical Transactions of the Royal Society B: Biological Sciences 364, 1789–1801. doi:10.1098/rstb.2008.0273

Meehan, M.L., Barreto, C., Turnbull, M.S., Bradley, R.L., Bellenger, J.-P., Darnajoux, R., Lindo, Z., 2020. Response of soil fauna to simulated global change factors depends on ambient climate conditions. Pedobiologia 83, 150672. doi:https://doi.org/10.1016/j.pedobi.2020.150672

Meehan, M.L., Caruso, T., Lindo, Z., 2021. Short-term intensive warming shifts predator communities (Parasitiformes: Mesostigmata) in boreal forest soils. Pedobiologia 87–88, 150742. doi:https://doi.org/10.1016/j.pedobi.2021.150742

Moore, J.C., de Ruiter, P.C., 2012. Energetic Food Webs: an Analysis of Real and Model Ecosystems, 1st Edition. ed. Oxford University Press, Oxford, UK.

Neutel, A.-M., Heesterbeek, J.A.P., Ruiter, P., 2002. Stability in real food webs: weak links in long loops. Science 296, 1120–1123. doi:10.1126/science.1068326

O'Gorman, E.J., Emmerson, M.C., 2009. Perturbations to trophic interactions and the stability of complex food webs. PNAS 106, 13393–13398. doi:https://doi.org/10.1073/pnas.0903682106

Oksanen, J., Blanchet, F.G., Friendly, M., Kindt, R., Legendre, P., McGlinn, D., Minchin, P.R., O'Hara, R.B., Simpson, G.L., Solymos, P., Stevens, M.H.H., Szoecs, E., Wagner, H., 2020. vegan: Community Ecology Package. R package version 2.5-7. [WWW Document]. URL https://CRAN.R-project.org/package=vegan (accessed 7.9.23).

Palozzi, J.E., Lindo, Z., 2017. Boreal peat properties link to plant functional traits of ecosystem engineers. Plant and Soil 418, 277–291. doi:10.1007/s11104-017-3291-0

Parimuchová, A., Dušátková, L.P., Kováč, Ľ., Macháčková, T., Slabý, O., Pekár, S., 2021. The food web in a subterranean ecosystem is driven by intraguild predation. Scientific Reports 11, 4994. doi:10.1038/s41598-021-84521-1

Perkins-Kirkpatrick, S.E., Lewis, S.C., 2020. Increasing trends in regional heatwaves. Nature Communications 11. doi:10.1038/s41467-020-16970-7

Persson, T., Lohm, U., 1977. Energetical significance of the annelids and arthropods in a swedish grassland soil. Ecological Bulletins.

Peschel, K., Norton, R.A., Scheu, S., Maraun, M., 2006. Do oribatid mites live in enemy-free space? Evidence from feeding experiments with the predatory mite *Pergamasus septentrionalis*. Soil Biology and Biochemistry 38, 2985–2989. doi:10.1016/J.SOILBIO.2006.04.035

Peterson, M.E., Daniel, R.M., Danson, M.J., Eisenthal, R., 2007. The dependence of enzyme activity on temperature: Determination and validation of parameters. Biochemical Journal 402, 331–337. doi:10.1042/BJ20061143

Pfingstl, T., Schatz, H., 2021. A survey of lifespans in Oribatida excluding Astigmata (Acari). Zoosymposia 20. doi:10.11646/zoosymposia.20.1.4

Price, D.T., Alfaro, R.I., Brown, K.J., Flannigan, M.D., Fleming, R.A., Hogg, E.H., Girardin, M.P., Lakusta, T., Johnston, M., McKenney, D.W., Pedlar, J.H., Stratton, T., Sturrock, R.N., Thompson, I.D., Trofymow, J.A., Venier, L.A., 2013. Anticipating the consequences of climate change for Canada's boreal forest ecosystems1. Environmental Reviews. doi:10.1139/er-2013-0042

Rillig, M.C., Ryo, M., Lehmann, A., Aguilar-Trigueros, C.A., Buchert, S., Wulf, A., Iwasaki, A., Roy, J., Yang, G., 2019. The role of multiple global change factors in driving soil functions and microbial biodiversity. Science 366, 886–890. doi:10.1126/science.aay2832

Rooney, N., McCann, K., Gellner, G., Moore, J.C., 2006. Structural asymmetry and the stability of diverse food webs. Nature 442, 265–269. doi:10.1038/nature04887

Saiya-Cork, K.R., Sinsabaugh, R.L., Zak, D.R., 2002. The effects of long term nitrogen deposition on extracellular enzyme activity in an *Acer saccharum* forest soil. Soil Biology and Biochemistry 34, 1309–1315. doi:10.1016/S0038-0717(02)00074-3

Schuur, E.A., Matson, P.A., 2001. Net primary productivity and nutrient cycling across a mesic to wet precipitation gradient in Hawaiian montane forest. Oecologia 128, 431–442. doi:10.1007/s004420100671

Schwarz, B., Barnes, A., Thakur, M., Brose, U., Ciobanu, M., Reich, P., Rich, R., Rosenbaum, B., Stefanski, A., Eisenhauer, N., 2017. Warming alters energetic structure and function but not resilience of soil food webs. Nature Climate Change 7, 895–900. doi:10.1038/s41558-017-0002-z

Seneviratne, S.I., Corti, T., Davin, E.L., Hirschi, M., Jaeger, E.B., Lehner, I., Orlowsky, B., Teuling, A.J., 2010. Investigating soil moisture–climate interactions in a changing climate: A review. Earth-Science Reviews 99, 125–161. doi:10.1016/J.EARSCIREV.2010.02.004

Shackelford, G.E., Haddaway, N.R., Usieta, H.O., Pypers, P., Petrovan, S.O., Sutherland, W.J., 2018. Cassava farming practices and their agricultural and environmental impacts: a systematic map protocol. Environmental Evidence 7, 30. doi:10.1186/s13750-018-0142-2

Sharma, Rahul, Prakash, O., Sonawane, M.S., Nimonkar, Y., Golellu, P.B., Sharma, Rohit, 2016. Diversity and distribution of phenol oxidase producing fungi from Soda Lake and description of *Curvularia lonarensis* sp. nov. Frontiers in Microbiology 7. doi:10.3389/fmicb.2016.01847

Sinsabaugh, R.L., 2010. Phenol oxidase, peroxidase and organic matter dynamics of soil. Soil Biology and Biochemistry 42, 391–404. doi:10.1016/J.SOILBIO.2009.10.014

Staddon, P., Lindo, Z., Crittenden, P.D., Gilbert, F., Gonzalez, A., 2010. Connectivity, non-random extinction and ecosystem function in experimental metacommunities. Ecology Letters 13, 543–552. doi:https://doi.org/10.1111/j.1461-0248.2010.01450.x

Starzomski, B.M., Srivastava, D.S., 2007. Landscape geometry determines community response to disturbance. Oikos 116, 690–699. doi:https://doi.org/10.1111/j.0030-1299.2007.15547.x

Sylvain, Z.A., Wall, D.H., Cherwin, K.L., Peters, D.P.C., Reichmann, L.G., Sala, O.E., 2014. Soil animal responses to moisture availability are largely scale, not ecosystem dependent: Insight from a cross-site study. Global Change Biology 20, 2631–2643. doi:10.1111/gcb.12522

Tarnocai, C., Canadell, J.G., Schuur, E.A.G., Kuhry, P., Mazhitova, G., Zimov, S., 2009. Soil organic carbon pools in the northern circumpolar permafrost region. Global Biogeochemical Cycles 23. doi:https://doi.org/10.1029/2008GB003327

Teng, J., McCann, K.S., 2004. Dynamics of compartmented and reticulate food webs in relation to energetic flows. The American Naturalist 164, 85–100. doi:10.1086/421723

Thakur, M.P., van der Putten, W.H., Apon, F., Angelini, E., Vreš, B., Geisen, S., 2021. Resilience of rhizosphere microbial predators and their prey communities after an extreme heat event. Functional Ecology 35, 216–225. doi:10.1111/1365-2435.13696

Thompson, P.L., Isbell, F., Loreau, M., O'Connor, M.I., Gonzalez, A., 2018. The strength of the biodiversity–ecosystem function relationship depends on spatial scale. Proceedings of the Royal Society B: Biological Sciences 285. doi:10.1098/rspb.2018.0038

Tsiafouli, M.A., Kallimanis, A.S., Katana, E., Stamou, G.P., Sgardelis, S.P., 2005. Responses of soil microarthropods to experimental short-term manipulations of soil moisture. Applied Soil Ecology 29, 17–26. doi:10.1016/J.APSOIL.2004.10.002

Turnbull, M.S., Lindo, Z., 2015. Combined effects of abiotic factors on Collembola communities reveal precipitation may act as a disturbance. Soil Biology and Biochemistry 82, 36–43. doi:10.1016/J.SOILBIO.2014.12.007

Unger, I.M., Muzika, R.M., Motavalli, P.P., 2010. The effect of flooding and residue incorporation on soil chemistry, germination and seedling growth. Environmental and Experimental Botany 69, 113–120. doi:10.1016/J.ENVEXPBOT.2010.03.005

Verhoef, H.A., Brussaard, L., 1990. Decomposition and nitrogen mineralization in natural and agroecosystems: the contribution of soil animals. Biogeochemistry 11, 175–211. doi:10.1007/BF00004496

Visser, E.J.W., Voesenek, L.A.C.J., 2005. Acclimation to soil flooding-sensing and signal-transduction. Plant and Soil 274, 197–214. doi:10.1007/s11104-004-1650-0

Webster, K.L., McLaughlin, J.W., Kim, Y., Packalen, M.S., Li, C.S., 2013. Modelling carbon dynamics and response to environmental change along a boreal fen nutrient gradient. Ecological Modelling 248, 148–164. doi:10.1016/J.ECOLMODEL.2012.10.004

Weltzin, J.F., Pastor, J., Harth, C., Bridgham, S.D., Updegraff, K., Chapin, C.T., 2000. Response of bog and fen plant communities to warming and water-table manipulations. Ecology 81, 3464–3478. doi:10.1890/0012-9658(2000)081[3464:ROBAFP]2.0.CO;2

Weston, C.J., Whittaker, K.L., 2004. Soil Biology and Tree Growth | Soil Biology. Encyclopedia of Forest Sciences 1183–1189. doi:10.1016/B0-12-145160-7/00248-9

Xu, G., Lu, H., Zhang, J., Shi, L., Yu, S., Chen, J., Mo, L., Wu, Z., Fu, S., 2022. Unexpected reduction of soil mesofauna under canopy N deposition in a subtropical forest. Forest Ecology and Management 504, 119738. doi:https://doi.org/10.1016/j.foreco.2021.119738

Zhang, H., Väliranta, M., Swindles, G.T., Aquino-López, M.A., Mullan, D., Tan, N., Amesbury, M., Babeshko, K. V., Bao, K., Bobrov, A., Chernyshov, V., Davies, M.A., Diaconu, A.C., Feurdean, A., Finkelstein, S.A., Garneau, M., Guo, Z., Jones, M.C., Kay, M., Klein, E.S., Lamentowicz, M., Magnan, G., Marcisz, K., Mazei, N., Mazei, Y., Payne, R., Pelletier, N., Piilo, S.R., Pratte, S., Roland, T., Saldaev, D., Shotyk, W., Sim, T.G., Sloan, T.J., Słowiński, M., Talbot, J., Taylor, L., Tsyganov, A.N., Wetterich, S., Xing, W., Zhao, Y., 2022. Recent climate change has driven divergent hydrological shifts in high-latitude peatlands. Nature Communications 13. doi:10.1038/s41467-022-32711-4

Appendices

Appendix A. Node model parameters for the soil food web trophic groups under control (12 °C) and warmed (20 °C) conditions.

Parameters include C:N and estimated percent assimilation efficiency (E_a), percent production efficiency (E_p), and population death rates (d).[1,2,3]

		Control (12 °C)			Warming (20 °C)		
Node ID	C:N	E_a	E_p	d	E_a	E_p	d
Arthropod feeding mites	8	60	35	1.84	60	31	2.44
Nematode-feeding mites	8	90	35	1.84	90	31	2.44
Non-predatory prostigmatid and astigmatid mites	8	50	35	1.84	50	31	2.44
Juvenile oribatid mites	8	50	35	1.2	50	31	1.59
Adult oribatid mites	8	50	35	1.2	50	31	1.59
Collembola	8	50	35	1.84	50	31	2.44
Predatory nematodes	10	50	37	1.6	50	33	2.13
Bactivorous nematodes	10	60	37	4.36	60	33	5.79
Fungivorous nematodes	10	38	37	1.92	38	33	2.55
Omnivorous nematodes	10	60	37	2.68	60	33	3.56
Protists	7	95	40	6	95	37	8.03
Bacteria	4	100	30	6	100	28	8.03
Fungi	10	100	30	1.2	100	28	1.61
Labile detritus	57	100	100	0	100	100	0
Recalcitrant detritus	19	100	100	0	100	100	0

[1]Metabolic parameters from Hunt et al. (1987).
[2]Metabolic scaling of parameters for microbial nodes from Li et al. (2019).
[3]Metabolic scaling of parameters for soil fauna nodes from Luxton (1972, 1981).

Appendix B. The soil food web interaction matrix.

Rows denote consumers, columns denote resources. A value of 1 indicates the presence of a trophic interaction, and a value of 0 indicates no interaction. Values greater than 0 but less than 1 indicate the presence of a weak trophic interaction. Meso = arthropod-feeding mites, Zerco = nematode-feeding mites, Mites NP = non-predatory prostigmatid and astigmatid mites, Col = collembola, Pred Nem = predatory nematodes, Bac Nem = bactivorous nematodes, Fung Nem = fungivorous nematodes, Omni Nem = omnivorous nematodes, Pro = protists, Bact = bacteria, Fung = fungi, Labile = labile detritus, Recal = recalcitrant detritus.

Node ID	Meso	Zerco	Mites NP	Juv Orib	Orib	Coll	Pred Nem	Bac Nem	Fung Nem	Omni Nem	Pro	Bact	Fung	Labile	Recal
Meso	0	0	1	1	0	1	0	0	0	0	0	0	0	0	0
Zerco	0	0	0	0	0	0	1	1	1	1	0	0	0	0	0
Mites NP	0	0	0	0	0	0	0	0	0	0	0	0	0	0	0
Juv Orib	0	0	0	0	0	0	0	0	0	0	0	0	1	0	0
Orib	0	0	0	0	0	0	0	0	0	0	0	0	1	0	0
Coll	0	0	0	0	0	0	0	0	0	0	0	0	1	0	0
Pred Nem	0	0	0	0	0	0	0	1	1	1	1	0	0	0	0
Bact Nem	0	0	0	0	0	0	0	0	0	0	1	1	0	0	0
Fung Nem	0	0	0	0	0	0	0	0	0	0	0	0	1	0	0
Omni Nem	0	0	0	0	0	0	0.5	0.5	0.5	0	1	1	1	0	0
Protists	0	0	0	0	0	0	0	0	0	0	0	1	0	0	0
Bacteria	0	0	0	0	0	0	0	0	0	0	0	0	0	0.3	0.7
Fungi	0	0	0	0	0	0	0	0	0	0	0	0	0	0.7	0.3

Appendix C. Mean node biomasses.

Biomasses (± SE) are given in g of C per m^2 of soil under each experimental treatment. Meso = arthropod-feeding mites, Zerco = nematode-feeding mites, Mites NP = non-predatory prostigmatid and astigmatid mites, Col = collembola, Pred Nem = predatory nematodes, Bac Nem = bactivorous nematodes, Fung Nem = fungivorous nematodes, Omni Nem = omnivorous nematodes, Pro = protists, Bact = bacteria, Fung = fungi, Labile = labile detritus, Recal = recalcitrant detritus.

Treatment	Meso	Zerco	Mites NP	Juv Orib	Orib	Coll	Pred Nem	Bac Nem	Fung Nem	Omni Nem	Pro	Bact	Fung	Labile	Recal
T_0	0.003 ± 0.002	0.009 ± 0.004	0.041 ± 0.008	0.31 ± 0.04	0.36 ± 0.04	0.004 ± 0.002	0.0019 ± 0.0004	0.0006 ± 0.0002	0.0060 ± 0.0014	0.0007 ± 0.0002	2.8 ± 0.1	11.7 ± 0.2	87 ± 2	135707	135707
T_1 Field-moist 12 °C	0.006 ± 0.002	0.005 ± 0.003	0.040 ± 0.016	0.14 ± 0.03	0.29 ± 0.05	0.006 ± 0.004	0.0013 ± 0.0009	0.0005 ± 0.0003	0.0043 ± 0.0029	0.0005 ± 0.0003	2.5 ± 0.1	10.6 ± 0.6	79 ± 4	135707	135707
T_2 Field-moist 12 °C	0.002 ± 0.001	0.003 ± 0.001	0.035 ± 0.010	0.13 ± 0.03	0.21 ± 0.04	0.004 ± 0.002	0.0014 ± 0.0004	0.0005 ± 0.0001	0.0046 ± 0.0013	0.0005 ± 0.0001	2.3 ± 0.1	9.9 ± 0.5	74 ± 4	135707	135707
T_1 Saturated 12 °C	0.001 ± 0.001	0.006 ± 0.003	0.027 ± 0.005	0.07 ± 0.02	0.14 ± 0.04	0.000 ± 0.000	0.0005 ± 0.0002	0.0002 ± 0.0001	0.0017 ± 0.0005	0.0002 ± 0.0001	2.7 ± 0.1	11.6 ± 0.3	86 ± 2	135707	135707
T_2 Saturated 12 °C	0.004 ± 0.002	0.004 ± 0.002	0.030 ± 0.006	0.10 ± 0.02	0.20 ± 0.04	0.002 ± 0.002	0.0006 ± 0.0002	0.0002 ± 0.0001	0.0019 ± 0.0005	0.0002 ± 0.0001	2.6 ± 0.1	11.1 ± 0.5	82 ± 4	135707	135707
T_1 Field-moist 20 °C	0.010 ± 0.005	0.008 ± 0.004	0.091 ± 0.047	0.17 ± 0.05	0.32 ± 0.06	0.011 ± 0.008	0.0029 ± 0.0013	0.0010 ± 0.0004	0.0092 ± 0.0041	0.0011 ± 0.0005	2.6 ± 0.1	10.9 ± 0.3	81 ± 3	135707	135707
T_2 Field-moist 20 °C	0.002 ± 0.001	0.004 ± 0.002	0.032 ± 0.011	0.09 ± 0.02	0.17 ± 0.02	0.002 ± 0.001	0.0018 ± 0.0004	0.0006 ± 0.0001	0.0057 ± 0.0012	0.0007 ± 0.0001	2.5 ± 0.1	10.6 ± 0.2	79 ± 2	135707	135707
T_1 Saturated 20 °C	0.004 ± 0.003	0.003 ± 0.002	0.030 ± 0.010	0.12 ± 0.02	0.20 ± 0.06	0.002 ± 0.001	0.0006 ± 0.0001	0.0002 ± 0.0001	0.0018 ± 0.0005	0.0002 ± 0.0001	2.7 ± 0.1	11.6 ± 0.3	86 ± 2	135707	135707
T_2 Saturated 20 °C	0.002 ± 0.001	0.002 ± 0.002	0.023 ± 0.006	0.10 ± 0.04	0.18 ± 0.07	0.001 ± 0.001	0.0003 ± 0.0001	0.0001 ± 0.0001	0.0008 ± 0.0002	0.0001 ± 0.0001	2.7 ± 0.1	11.3 ± 0.2	84 ± 2	135707	135707

Appendix D. Supplementary table of means.

Mean value (± SE) for each variable measured. Heterotrophic respiration is given in ln(g of C per m^2 per year); soil moisture is given in ln(percent) gravimetrically; pH is given in ln(pH); C:N ratio is a unitless quantity; phenol oxidase and peroxidase concentration is given in μmol substrate per g soil per hour; total abundance and microfauna abundance is given in individuals per m^2; mesofauna abundance is given in ln(individuals per m^2); total biomass is given in in g of C per m^2; consumptive flux and C mineralization are given in g of C per m^2 per year; N mineralization is given in g of N per m^2 per year.

	T_0	T_1 Field-moist 12 °C	T_2 Field-moist 12 °C	T_1 Saturated 12 °C	T_2 Saturated 12 °C	T_1 Field-moist 20 °C	T_2 Field-moist 20 °C	T_1 Saturated 20 °C	T_2 Saturated 20 °C
Heterotrophic Respiration	7.0 ± 0.2	6.0 ± 0.4	6.1 ± 0.3	6.4 ± 0.5	6.7 ± 0.4	6.7 ± 0.5	6.7 ± 0.4	7.0 ± 0.2	6.8 ± 0.5
Soil Moisture	6.68 ± 0.13	6.68 ± 0.09	6.72 ± 0.07	6.94 ± 0.07	6.84 ± 0.06	6.64 ± 0.08	6.57 ± 0.07	6.86 ± 0.07	6.83 ± 0.07
pH	1.405 ± 0.013	1.414 ± 0.010	1.443 ± 0.022	1.424 ± 0.010	1.447 ± 0.014	1.378 ± 0.004	1.436 ± 0.013	1.414 ± 0.015	1.445 ± 0.009
C:N	37 ± 2	36 ± 3	33 ± 3	36 ± 3	36 ± 1	40 ± 5	39 ± 3	38 ± 2	33 ± 2
Phenol oxidase	160 ± 16	131 ± 29	146 ± 8	90 ± 19	160 ± 8	199 ± 24	155 ± 8	183 ± 31	148 ± 5
Peroxidase	154 ± 8	111 ± 36	172 ± 13	98 ± 21	183 ± 9	143 ± 12	175 ± 24	157 ± 16	163 ± 15
Total Abundance	540,000 ± 50,000	330,000 ± 130,000	300,000 ± 60,000	150,000 ± 30,000	200,000 ± 40,000	360,000 ± 70,000	290,000 ± 40,000	220,000 ± 50,000	160,000 ± 50,000
Microfauna Abundance	170,000 ± 40,000	120,000 ± 80,000	130,000 ± 40,000	50,000 ± 10,000	50,000 ± 20,000	260,000 ± 120,000	160,000 ± 40,000	50,000 ± 10,000	20,000 ± 10,000
Mesofauna Abundance	12.8 ± 0.1	12.1 ± 0.2	12.0 ± 0.2	11.4 ± 0.2	11.8 ± 0.2	12.4 ± 0.4	11.7 ± 0.2	11.9 ± 0.2	11.6 ± 0.3
Total Biomass	0.74 ± 0.08	0.49 ± 0.10	0.40 ± 0.08	0.25 ± 0.07	0.34 ± 0.07	0.46 ± 0.09	0.31 ± 0.05	0.37 ± 0.09	0.31 ± 0.11
Microfauna Biomass	0.0092 ± 0.0022	0.0066 ± 0.0044	0.0070 ± 0.0020	0.0026 ± 0.0008	0.0029 ± 0.0008	0.0080 ± 0.0017	0.0087 ± 0.0019	0.0028 ± 0.0007	0.0013 ± 0.0004
Mesofauna Biomass	0.73 ± 0.08	0.48 ± 0.10	0.39 ± 0.08	0.25 ± 0.07	0.34 ± 0.07	0.46 ± 0.09	0.30 ± 0.05	0.36 ± 0.09	0.31 ± 0.11
Consumptive flux	1261 ± 4	1214 ± 65	1127 ± 54	1309 ± 32	1254 ± 52	1863 ± 69	1205 ± 27	1967 ± 60	1280 ± 28
C mineralization	514 ± 2	496 ± 27	461 ± 22	535 ± 13	513 ± 21	776 ± 29	492 ± 11	820 ± 25	523 ± 11
N mineralization	-4.69 ± 0.04	-4.67 ± 0.26	-4.39 ± 0.22	-3.18 ± 0.22	-4.77 ± 0.13	-5.25 ± 0.09	-4.95 ± 0.24	-3.52 ± 0.10	-5.10 ± 0.12

Appendix E. Supplementary table of ANOVA outputs.

ANOVA output for each variable measured. Heterotrophic respiration is given in ln(g of C per m^2 per year); soil moisture is given in ln(percent) gravimetrically; pH is given in ln(pH); C:N ratio is a unitless quantity; phenol oxidase and peroxidase concentration is given in μmol substrate per g soil per hour; total abundance and microfauna abundance is given in individuals per m^2; mesofauna abundance is given in ln(individuals per m^2); total biomass is given in in g of C per m^2; consumptive flux and C mineralization are given in g of C per m^2 per year; N mineralization is given in g of N per m^2 per year.

	Intercept	Soil Moisture Treatment	Temperature Treatment	Destructive Sampling Treatment	Block Effect	Soil Moisture x Temperature Interaction	Soil Moisture x Destructive Sampling Interaction	Temperature x Destructive Sampling Interaction	Soil Moisture x Temperature x Destructive Sampling Interaction
Soil Moisture	$F_{1,32} = 17022.446$; $p < 0.001$	$F_{1,32} = 18.407$; $p < 0.001$	$F_{1,32} = 1.856$; $p = 0.183$	$F_{1,32} = 0.695$; $p = 0.411$	$F_{1,32} = 0.159$; $p = 0.693$	–	–	–	–
Soil pH	$F_{1,32} = 17476.702$; $p < 0.001$	$F_{1,32} = 2.097$; $p = 0.157$	$F_{1,32} = 1.630$; $p = 0.211$	$F_{1,32} = 12.166$; $p = 0.001$	$F_{1,32} = 0.028$; $p = 0.868$	–	–	–	–
C:N	$F_{1,31} = 336.769$; $p < 0.001$	$F_{1,31} = 0.398$; $p = 0.533$	$F_{1,31} = 1.522$; $p = 0.227$	$F_{1,31} = 0.502$; $p = 0.484$	$F_{1,31} = 1.038$; $p = 0.316$	–	–	–	–
Phenol Oxidase Activity	$F_{1,32} = 55.547$; $p < 0.001$	$F_{1,32} = 0.760$; $p = 0.390$	$F_{1,32} = 16.455$; $p < 0.001$	$F_{1,32} = 5.398$; $p = 0.027$	$F_{1,32} = 1.159$; $p = 0.290$	–	–	$F_{1,32} = 9.001$; $p = 0.005$	–
Peroxidase Activity	$F_{1,31} = 34.176$; $p < 0.001$	$F_{1,31} = 0.009$; $p = 0.925$	$F_{1,31} = 6.955$; $p = 0.013$	$F_{1,31} = 20.949$; $p < 0.001$	$F_{1,31} = 6.091$; $p = 0.019$	–	–	$F_{1,31} = 5.235$; $p = 0.029$	–
Heterotrophic Respiration	$F_{1,34} = 139.272$; $p < 0.001$	$F_{1,34} = 1.670$; $p = 0.205$	$F_{1,34} = 3.975$; $p = 0.054$	$F_{1,34} = 0.109$; $p = 0.743$	$F_{1,34} = 0.243$; $p = 0.625$	–	–	–	–
Total Fauna Abundance	$F_{1,34} = 57.927$; $p < 0.001$	$F_{1,34} = 19.104$; $p < 0.001$	$F_{1,34} = 0.509$; $p = 0.481$	$F_{1,34} = 0.466$; $p = 0.499$	$F_{1,34} = 22.953$; $p < 0.001$	–	–	–	–
Microfauna Abundance	$F_{1,34} = 23.738$; $p < 0.001$	$F_{1,34} = 21.152$; $p < 0.001$	$F_{1,34} = 0.403$; $p = 0.530$	$F_{1,34} = 0.966$; $p = 0.333$	$F_{1,34} = 11.168$; $p = 0.002$	–	–	–	–
Mesofauna Abundance	$F_{1,33} = 4938.218$; $p < 0.001$	$F_{1,33} = 6.143$; $p = 0.018$	$F_{1,33} = 2.821$; $p = 0.103$	$F_{1,33} = 1.968$; $p = 0.170$	$F_{1,33} = 11.936$; $p = 0.002$	–	–	$F_{1,33} = 4.276$; $p = 0.047$	–
Total Fauna Biomass	$F_{1,33} = 58.915$; $p < 0.001$	$F_{1,33} = 8.631$; $p = 0.006$	$F_{1,33} = 0.076$; $p = 0.784$	$F_{1,33} = 1.375$; $p = 0.249$	$F_{1,33} = 17.288$; $p < 0.001$	–	$F_{1,33} = 3.386$; $p = 0.075$	–	–
Microfauna Biomass	$F_{1,34} = 23.738$; $p < 0.001$	$F_{1,34} = 21.152$; $p < 0.001$	$F_{1,34} = 0.403$; $p = 0.530$	$F_{1,34} = 0.966$; $p = 0.333$	$F_{1,34} = 11.168$; $p = 0.002$	–	–	–	–
Mesofauna Biomass	$F_{1,33} = 57.804$; $p < 0.001$	$F_{1,33} = 8.266$; $p = 0.007$	$F_{1,33} = 0.069$; $p = 0.795$	$F_{1,33} = 1.440$; $p = 0.239$	$F_{1,33} = 16.758$; $p < 0.001$	–	$F_{1,33} = 3.439$; $p = 0.073$	–	–
Total Consumption	$F_{1,33} = 1046.791$; $p < 0.001$	$F_{1,33} = 8.653$; $p = 0.006$	$F_{1,33} = 214.881$; $p < 0.001$	$F_{1,33} = 0.748$; $p = 0.393$	$F_{1,33} = 6.267$; $p = 0.017$	–	–	$F_{1,33} = 94.744$; $p < 0.001$	–
C Mineralization	$F_{1,33} = 1030.642$; $p < 0.001$	$F_{1,33} = 8.725$; $p = 0.006$	$F_{1,33} = 236.901$; $p < 0.001$	$F_{1,33} = 0.739$; $p = 0.396$	$F_{1,33} = 6.173$; $p = 0.018$	–	–	$F_{1,33} = 105.313$; $p < 0.001$	–
N Mineralization	$F_{1,33} = 1047.625$; $p < 0.001$	$F_{1,33} = 13.061$; $p = 0.001$	$F_{1,33} = 78.383$; $p < 0.001$	$F_{1,33} = 2.387$; $p = 0.132$	$F_{1,33} = 0.002$; $p = 0.965$	–	–	$F_{1,33} = 54.875$; $p < 0.001$	–

Appendix F. Supplementary table of linear model outputs.

Estimate of coefficient (± SEM) for each variable measured, based on corresponding linear models. Heterotrophic respiration is given in ln(g of C per m^2 per year); soil moisture is given in ln(percent) gravimetrically; pH is given in ln(pH); C:N ratio is a unitless quantity; phenol oxidase and peroxidase concentration is given in μmol substrate per g soil per hour; total abundance and microfauna abundance is given in individuals per m^2; mesofauna abundance is given in ln(individuals per m^2); total biomass is given in in g of C per m^2; consumptive flux and C mineralization are given in g of C per m^2 per year; N mineralization is given in g of N per m^2 per year.

	Intercept	Saturated Soil Moisture	+ 8 °C Warming	T_2 Destructive Sampling	High Abundance Block	Saturated Soil Moisture x + 8 °C Warming	Saturated Soil Moisture x T_2 Destructive Sampling	+ 8 °C Warming x T_2 Destructive Sampling	Saturated Soil Moisture x + 8 °C Warming x T_2 Destructive Sampling
Soil Moisture	6.71 ± 0.05	0.21 ± 0.05	-0.07 ± 0.05	-0.04 ± 0.05	-0.04 ± 0.10	–	–	–	–
Soil pH	1.406 ± 0.011	0.014 ± 0.010	-0.012 ± 0.010	0.036 ± 0.010	0.003 ± 0.019	–	–	–	–
C:N	36 ± 2	-1 ± 2	2 ± 2	-1 ± 2	4 ± 4	–	–	–	–
Phenol Oxidase Activity	110 ± 20	-10 ± 10	80 ± 20	40 ± 20	30 ± 30	–	–	-80 ± 30	–
Peroxidase Activity	96 ± 15	1 ± 12	47 ± 18	81 ± 18	68 ± 28	–	–	-55 ± 24	–
Heterotrophic Respiration	6.30 ± 0.53	0.36 ± 0.28	0.55 ± 0.28	0.09 ± 0.29	0.27 ± 0.54	–	–	–	–
Total Fauna Abundance	280,000 ± 40,000	-150,000 ± 30,000	20,000 ± 30,000	20,000 ± 40,000	330,000 ± 70,000	–	–	–	–
Microfauna Abundance	110,000 ± 20,000	-100,000 ± 20,000	10,000 ± 20,000	20,000 ± 20,000	150,000 ± 40,000	–	–	–	–
Mesofauna Abundance	11.8 ± 0.2	-0.4 ± 0.1	0.4 ± 0.2	0.3 ± 0.2	1.0 ± 0.3	–	–	-0.6 ± 0.3	–
Total Fauna Biomass	0.43 ± 0.06	-0.20 ± 0.07	0.01 ± 0.05	-0.08 ± 0.07	0.40 ± 0.10	–	0.18 ± 0.10	–	–
Microfauna Biomass	0.0061 ± 0.0012	-0.0056 ± 0.0012	0.0008 ± 0.0012	0.0012 ± 0.0013	0.0079 ± 0.0024	–	–	–	–
Mesofauna Biomass	0.42 ± 0.06	-0.20 ± 0.07	0.01 ± 0.05	-0.08 ± 0.07	0.39 ± 0.09	–	0.18 ± 0.10	–	–
Total Consumption	1180 ± 40	90 ± 30	670 ± 50	-40 ± 50	160 ± 60	–	–	-620 ± 60	–
C Mineralization	484 ± 15	39 ± 13	289 ± 19	-16 ± 19	64 ± 26	–	–	-268 ± 26	–
N Mineralization	-4.73 ± 0.15	-0.46 ± 0.13	1.61 ± 0.18	0.28 ± 0.18	-0.01 ± 0.25	–	–	-1.87 ± 0.25	–

Curriculum Vitae

Name:	Trevor Pettit
Post-secondary Education and Degrees:	Western University London, Ontario, Canada 2016-2021 B.Sc. Western University London, Ontario, Canada 2021-2023 M.Sc.
Honours and Awards:	Province of Ontario Graduate Scholarship 2022-2023 Canadian Society of Ecology and Evolution Travel Award 2023 OE3C Colloquium Travel Award 2023
Related Work Experience	Teaching Assistant The University of Western Ontario 2021-2023

Publications and Presentations:

Pettit, T., Faulkner, K.J., Buchkowski, R.W., Kamath, D., and Lindo, Z. (2023) Changes in peatland soil fauna biomass alter food web structure and function under warming and hydrological changes. European Journal of Soil Biology 117: 103509. https://doi.org/10.1016/j.ejsobi.2023.103509

Pettit, T., Faulkner, K.J., Buchkowski, R.W., Kamath, D., and Lindo, Z. (2023) Changes in peatland soil fauna biomass alter food web structure and function under warming and hydrological changes. Canadian Society of Ecology and Evolution General Annual Meeting. Winnipeg, MB.

Pettit, T., Faulkner, K.J., Buchkowski, R.W., Kamath, D., and Lindo, Z. (2023) Changes in peatland soil fauna biomass alter food web structure and function under warming and hydrological changes. Ontario Ecology, Ethology, and Evolution Colloquium. London, ON.